Computers and Chemical Engineering 181 (2024) 108548

Contents lists available at ScienceDirect

Computers and Chemical Engineering

journal homepage: www.elsevier.com/locate/cace

# Modeling robust bi-level BCC production planning problem with uncertain carbon emission mechanism

Jia Zhao [a,1], Yankui Liu [b,1], Aixia Chen [c,*]

[a] Risk Management & Financial Engineering Laboratory, College of Mathematics & Information Science, Hebei University, Baoding, 071002, Hebei, China
[b] Hebei Key Laboratory of Machine Learning and Computational Intelligence, College of Mathematics & Information Science, Hebei University, Baoding, 071002, Hebei, China
[c] School of Management, Hebei University, Baoding, 071002, Hebei, China

ARTICLE INFO

*Keywords:*
Biomass–coal co-firing
Carbon emission
Bi-level programming
Lagrange duality
Uncertainty set

ABSTRACT

This paper studies the biomass–coal co-firing (BCC) production planning problem under the carbon emission quota allocation (CEQA) mechanism. However, carbon emission parameters are uncertain due to many factors, such as the type of power units and coal quality. To address this challenge issue, this paper proposes a new globalized robust bi-level optimization model, where the uncertain parameters are characterized by a pair of uncertainty sets. In the proposed model, the upper government as the leader decides the CEQA mechanism, while the lower power plants as the followers develop the production planning according to the given CEQA mechanism. Moreover, based on the Lagrange duality theory and Karush–Kuhn–Tucker (KKT) conditions, the proposed model is equivalently converted into a computationally tractable single-level model. Finally, a practical case study in Shandong Province demonstrates that compared with the nominal bi-level and robust bi-level models, the proposed optimization model can not only effectively resist parameter uncertainty, but also be less conservative.

## 1. Introduction

As the process of global industrialization accelerates, the energy consumption increases sharply, and the excessive greenhouse gas emissions cause an irreversible impact on the environment. The total global primary energy consumed by fuel increased to 595 exajoules in 2021, of which the coal played an important role and the total consumption reached 160 exajoules, accounting for 26.9% (Global, 2021). In the power generation sector, the coal plays an important role in the power plant fuel, accounting for 36% in 2021, owing to its low price and abundant production compared to other fuels. The 2021 global energy review of the $CO_2$ emissions reported that the global $CO_2$ emissions reached a critical point in 2021, with emissions from the industrial combustion rebounding to the highest level, reaching 36.3 gigatonnes (Global Energy Review, 2021). However, one of the prime reasons that the carbon emissions are so high is the coal power generation, which has led to the global warming and threatened human health globally (Oberschelp et al., 2019). In this situation, reducing the carbon emissions from the power plants becomes important. Research has shown that BCC power generation can effectively reduce the carbon emissions (Khademi and Ekşioğlu, 2021).

In addition, according to the structural characteristics of the biomass fuel, its high volatile content can improve the combustion efficiency, and thus improve the net thermal efficiency of the power plants (Fujishima et al., 2011). At present, the co-firing technology has been widely promoted, among which there are mainly three co-firing modes: (1) direct co-firing: it has lower requirements on the existing equipment of the power plant, but the biomass utilization efficiency is low; (2) indirect co-firing: its power generation efficiency is higher than the direct co-firing, and the existing coal-fired boiler equipment can be slightly modified for practical production; and (3) parallel co-firing: its fuel efficiency is higher than the above two modes, but it requires higher equipment (Sun et al., 2021). Therefore, the indirect co-firing is a relatively effective measure for the rectification of the existing power plants.

Notably, under the constraints of the carbon emission control, there is a hierarchical relationship between the government and power plants. As a public infrastructure, the power plants should be responsible for the impact of the economic sustainability and the social welfare under the supervision of the government (Zhu et al., 2020). Without government regulation, the power plants would not be responsible for their carbon emissions, which negatively impact the economic

* Corresponding author.
*E-mail addresses:* zhaojia_@stumail.hbu.edu.cn (J. Zhao), yliu@hbu.edu.cn (Y. Liu), chenaixia@hbu.edu.cn (A. Chen).
[1] Jia Zhao and Yankui Liu contributed equally to this work.

https://doi.org/10.1016/j.compchemeng.2023.108548
Received 26 August 2023; Received in revised form 4 November 2023; Accepted 6 December 2023
Available online 10 December 2023
0098-1354/

sustainability, and would only seek to maximize their profits (Jones et al., 2013). As a result, the objectives of the government and the power plants are conflicting. This motivates us to employ a bi-level optimization method to address this hierarchical relationship. As a leader, the government first allocates the carbon emission quotas to the power plants. Then, based on government decisions, the power plants develop their production plans.

In the past few years, research on the BCC models has attracted the attention of many scholars (Ekşioğlu et al., 2016; Cutz et al., 2019). In this respect, Ooi et al. (2022) proposed a mathematical model to study the optimal biofuel supply chain. A multi-objective mixed-integer linear programming model was constructed for the existing sugar factories that used the sugarcane bagasse for power generation (Varshney et al., 2019). Nevertheless, they did not consider the uncertainties in the power generation process of BCC.

The carbon emissions of the power plants are affected by various factors, which are unfavorable for decision-makers to obtain the exact values of the carbon emission parameters. Wang et al. (2022) studied the data of 30 provinces in China to develop some carbon emission reduction policies for the power generation industry, and identified the factors of the regional differences and driving factors. During the BCC power generation, the carbon emission parameters are mainly affected by the unit type, the coal burning quality and the operating load, so it is difficult for us to obtain the exact values of the carbon emission parameters. How should the decision-makers respond to this uncertainty?

In this paper, to handle uncertain carbon emission parameters, we use a pair of uncertainty sets to characterize the uncertain parameters. Accordingly, a globalized robust bi-level BCC model is formulated. In our model, the government, as the leader, decides the CEQA mechanism under the local socioeconomic and environmental conditions. The power plants, as the followers, develop the production plan according to the CEQA mechanism decided by the government. The contributions of this paper can be summarized in the following three aspects:

- Model: A new globalized robust bi-level optimization model is developed for the BCC planning problem under the carbon emission quota, where the uncertain carbon emission parameters are characterized by inner–outer uncertainty sets. The uncertain carbon emission parameters are contained in the lower level model, which pose a challenge in its solution method.
- Solvability: The proposed globalized robust bi-level BCC model is transformed into a computationally tractable system. Specifically, using Lagrange duality theory, the globalized robust constraint is converted to a convex constraint system. Furthermore, by replacing the lower-level model with its KKT conditions, we can obtain a single-level model which can be solved by commercial software.
- Application: The proposed model is applied to a real case about co-firing power plants in Shandong Province, China. The computational results lead to the conclusion that the globalized robust optimization (GRO) method can not only resist parameter uncertainty but also pay a lower price of robustness than robust optimization (RO) method.

The rest of paper is organized as follows: Section 2 presents the literature review. Section 3 further outlines the research problem in detail, proposes a globalized robust bi-level BCC optimization model under the CEQA mechanism. Section 4 converts the semi-infinite constraint into a finite system of convex constraints, and finally transforms the bi-level model into a single-level model. A case study about three power plants in Shandong Province is provided to verify the effectiveness and practicability of the globalized robust bi-level BCC optimization model in Section 5. Finally, Section 6 presents the conclusions.

## 2. Literature review

The literature review and the research gaps of this study are focused on in this section. The relevant literature review includes two aspects: the CEQA problem and uncertain BCC optimization models.

### 2.1. CEQA problem

The regional CEQA policy is considered to be an effective sustainable development policy to reduce the carbon emissions and increase the fiscal revenue (Zhou and Wang, 2016). For example, Yang and Lee (2022) proposed a CEQA mechanism, and the experimental results showed that the allocation mechanism played an important role in China's sustainable development, in which the carbon intensity was reduced by 6.69% and the economy was increased by 7026 billion RMB. Studies have shown that the carbon emission allowances are important to the regional economic growth and that the misallocation of the carbon allowances can have a negative impact on productivity and carbon performance.

In some areas, several studies have shown that the CEQA mechanism is an effective measure to reduce the carbon emissions. In the power industry, Zhang et al. (2018) proposed a general equilibrium model, and applied their model to practical cases, where the computational results showed that different carbon emission quota allocations can affect the price of electricity. When a CEQA scheme is implemented, there are usually two or more decision-makers. Based on the equilibrium strategy of the CEQA mechanism, a fuzzy optimization method was proposed to seek the tradeoff between the carbon emissions and the economy in the construction industry, and the method was applied to real cases (Zhao et al., 2018).

Both the free CEQA and taxable CEQA are discussed in this paper. According to Zhou et al. (2009) and Feng et al. (2018), the free CEQA refers to the carbon emission quota allocated by the government to power plants to keep them operating normally, while the taxable CEQA refers to the portion of carbon emissions that power plants apply to the government for additional quota over and above the free CEQA.

### 2.2. Uncertain BCC optimization models

There are many uncertain factors in the actual utilization of the biomass fuel. To address the uncertainty about the heating value and moisture content of biomass in the biomass supply chain, Shabani and Sowlati (2016) applied stochastic robust optimization to a multi-stage model, and the results showed that their method could prevent the adverse fluctuations caused by data uncertainty. For the biomass supply chain, Kim et al. (2011) presented an optimal design model of a biomass supply chain network under stochastic uncertainty. In addition, some researchers have studied the biomass supply chain in an uncertain environment (Samani and Hosseini-Motlagh, 2021; Awudu and Zhang, 2012; Soren and Shastri, 2019).

Generally, uncertain optimization methods include RO (Bertsimas and Sim, 2004; Ben-Tal et al., 2009), fuzzy optimization (FO), and stochastic optimization (SO). The FO method is applied to uncertain BCC optimization models, where the uncertain model parameters are characterized by possibility distributions. For instance, in an uncertain environment, Huang and Xu (2020) applied FO method to construct a bi-level multi-objective model for the sludge and coal co-firing power generation, which fully reflected the influence of fuzzy parameters on the modeling process. Due to the uncertainty of biomass supply prices, Chen and Liu (2023b) proposed a distributionally robust fuzzy location optimization model for biomass power plants. In addition, there are some other interesting work to use FO method to model BCC problem (Xu et al., 2018; Aviso et al., 2020; Lima et al., 2021).

In addition, many researchers have applied RO method to uncertain BCC optimization models. A RO model is presented to design the efficient biomass co-firing networks and determine the appropriate co-firing configurations and fuel mixtures (San Juan and Sy, 2022). To deal with uncertainties in biomass productivity and product sales prices, Theozzo and dos Santos (2023) proposed a RO model that allows for control of its conservatism. Chen and Liu (2023a) applied the GRO method to the biomass energy supply chain problem and demonstrated its superiority through practical cases.

**Table 1**
A review of the literature on uncertainty models.

| Researches | Model structure | | Uncertain parameters | | Optimization method | | | |
|---|---|---|---|---|---|---|---|---|
| | Single-level | Bi-level | Carbon emissions | Others | RO | FO | SO | GRO |
| Gebreslassie et al. (2012) | ✓ | | | ✓ | | | ✓ | |
| Xu et al. (2018) | | ✓ | | ✓ | | ✓ | | |
| Huang and Xu (2020) | | ✓ | ✓ | ✓ | | ✓ | | |
| Aviso et al. (2020) | ✓ | | | ✓ | | ✓ | | |
| Karimi et al. (2021) | ✓ | | | ✓ | | | ✓ | |
| San Juan and Sy (2022) | ✓ | | | ✓ | ✓ | | | |
| Aranguren and Castillo-Villar (2022) | ✓ | | | ✓ | | | ✓ | |
| Theozzo and dos Santos (2023) | ✓ | | | ✓ | ✓ | | | |
| This study | | ✓ | ✓ | | | | | ✓ |

The SO method also has many applications. In this respect, Karimi et al. (2021) took into account the uncertain emission factors in the process of the biomass–coal co-combustion power generation, and adopted the chance constraint to model uncertainty. Under uncertain supply and demand conditions, a multi-period, bi-criterion, stochastic mixed integer linear programming model was proposed to solve the optimization design and planning of the hydrocarbon biorefining supply chain (Gebreslassie et al., 2012). In addition, some researchers have applied SO method to uncertain biomass optimization problems (Aranguren and Castillo-Villar, 2022; Allman et al., 2021).

### 2.3. Research gaps

To illustrate the difference between this study and the existing literature, the literature related to the uncertain BCC optimization models is divided into three categories: model structure, uncertain parameters, and optimization methods, which are provided in Table 1, and the last line in the table shows the characteristics of our study.

In summary, the method proposed in this study is different from the existing literature, and the differences include the following three aspects:

- There are few studies that consider the hierarchical relationship between the government and power plants, and most existing literature use a single-level optimization model. In this paper, the CEQA mechanism is adopted and a bi-level optimization model is constructed considering the hierarchical relationship between the government and power plants.
- In the literature on bi-level models, FO methods are applied to address the uncertainty of the carbon emission parameters in the process of BCC power generation, while few studies apply GRO method to address the studied problem.
- In the existing robust bi-level optimization method, the uncertain parameters all present in the upper level model. However, in our study the uncertain carbon emission parameters are in the lower level model, which pose a challenge to model analysis.

The three aspects mentioned above demonstrate the originality and scientific merit in current study by comparing the related literature in the BCC problem.

## 3. Methodology

This section first introduces the BCC problem under the CEQA mechanism and then proposes a globalized robust bi-level optimization method for BCC problem.

### 3.1. Problem description

In the BCC problem under the CEQA mechanism, the government sets the CEQA at the upper level, and the power plants at the lower level determine their production plans according to the quotas set by the government. The government, as a representative of the public, is responsible for the sustainable development. The government not only controls the carbon emissions but also keeps the power plants running. Considering the social welfare and environmental protection, the government divides the CEQA into two parts. One part is the free CEQA, and second part is the taxable CEQA, which is paid to the government in the form of tax for the ecological compensation. To maximize the fiscal revenue, the government determines the CEQA to the power plants under the reducing carbon emission target, while the power plants create the production plan according to the government's CEQA and aim to maximize their profits.

Through the above analysis, the carbon emission quota plays a crux role in model construction. However, in the actual production process of the power plant, the carbon emission parameters are affected by many factors, including the type of power units, the quality of coal, and the operating load. These factors have a direct impact on the carbon emissions of the power plants, which in turn affects the excess carbon tax they pay to the government. Therefore, this paper considers uncertain carbon emission parameters and discusses the impacts of uncertainty on solution quality.

To clarify the research scope, some necessary assumptions involved in this paper are given as follows:

- Indirect co-firing is adopted in our BCC problem;
- Biomass and coal can be completely burned in a boiler;
- The production plan of the power plant is based on a one-year cycle.

To describe this model in detail, its associated notations and definition are given in Table A.1.

### 3.2. Model formulation

#### 3.2.1. Upper level model

For the sustainable development of the region, the government not only considers the long-term development of the economy but also takes responsibility for the environmental damage caused by the development process, and pays much attention to the carbon emissions which are mainly responsible for the greenhouse effect.

**Objective of the government: Maximizing tax revenue**

The government's potential fiscal revenue from the power plants mainly consists of two parts: the value-added tax and the tax revenue that exceeds the free CEQA. The value-added tax is $\rho \sum_{m=1}^{M} \sum_{n=1}^{N} [PPC_{mn}$

$(1-EC_{mn})-u_{mn}]z_{mn}$. Due to the excess carbon emissions, the tax revenue for the power plant is $w\sum_{m=1}^{M}y_m$. Combining these two parts, the objective function about the government tax revenue is:

$$\max \quad \text{GTR} = \rho\sum_{m=1}^{M}\sum_{n=1}^{N}[PPC_{mn}(1-EC_{mn})-u_{mn}]z_{mn}+w\sum_{m=1}^{M}y_m.$$

**Carbon intensity constraints:** The government proposes the carbon intensity constraints for all industries to achieve the sustainable development. The government achieves the carbon intensity constraints by restricting the allocation of the carbon emissions for the BCC power plants. The carbon emissions of the power plants divided by the electricity output provide the feedback on the carbon intensity indicators to the government. The coal-fired power plant's carbon intensity is $CI = \frac{\sum_{m=1}^{M}(x_m+y_m)}{\sum_{m=1}^{M}\sum_{n=1}^{N}PC_{mn}z_{mn}}$. To control the carbon emissions, the carbon intensity should be less than a certain value $r$, i.e.,

$$CI \leqslant r. \tag{1}$$

**Free carbon emission quota allocation proportion constraints:** On May 13, 2021, the Air Pollutant Emission Standard for Thermal Power Plants was reviewed and approved in principle at the executive meeting of the Ministry of Environmental Protection. The new standard has greatly improved the pollutant emission standard, which will further increase the cost pressure on the power plants, including the co-firing power plants. Consequently, the government should set the right proportion of the free carbon emissions to ensure the interests of the power plants and promote the ability of the power plants to improve their cleaner production. The free CEQA level can be expressed as $FP = \frac{x_m}{(x_m+y_m)}$. Let $\mu$ be the free CEQA level in conformity with the government's comprehensive decision o n the economy and society. Then the free CEQA proportion constraints can be shown as follows,

$$FP \geqslant \mu. \tag{2}$$

**The total carbon emissions constraint**: The government needs to set the carbon emissions cap to achieve the carbon reduction targets. The total CEQA constraint is represented as follows:

$$\sum_{m=1}^{M}(x_m+y_m) \leqslant \beta\ TEC, \tag{3}$$

where $\sum_{m=1}^{M}(x_m+y_m)$ denotes the total CEQA. As can be seen from the righthand of the total CEQA constraint, when the parameter TEC or $\beta$ increases, the total CEQA always increases.

**Operational requirements**: When formulating the carbon emission allocations, the government should ensure the basic operation of the lower-level power plants. In the meantime, the total CEQA cannot exceed the maximum full-load production for each power plant, which is represented as,

$$AQ_m^{min} \leqslant x_m + y_m \leqslant AQ_m^{max}, \forall m \in \mathcal{M}. \tag{4}$$

*3.2.2. Lower level model*

The lower power plants need to decide the production plan according to the government's carbon emission allocation mechanism and their aim to maximize profits. The lower level model will be constructed in the following.

**Objectives of the power plant: Maximizing profits**

The profit of the power plant comes from the electricity sold to the power supply enterprise. The cost of the power plant is mainly composed of four parts, the fuel cost, the garbage disposal cost, the tax cost, and the excess carbon emission cost. Therefore, the power plant profits are as follows:

$$\begin{aligned}\max \quad \text{PB}_m = & P\sum_{n=1}^{N}PC_{mn}(1-EC_{mn})z_{mn}-\sum_{n=1}^{N}u_{mn}z_{mn} \\ & -\sum_{n=1}^{N}\sum_{k=1}^{K}EP_{nk}TP_{nk}z_{mn}- \\ & \rho\sum_{m=1}^{M}\sum_{n=1}^{N}[PPC_{mn}(1-EC_{mn})-u_{mn}]z_{mn}-w\sum_{m=1}^{M}y_m-OC_m.\end{aligned}$$

**Uncertain carbon emissions amount constraints:** From the power plant's point of view, it cannot exceed the total carbon emissions set by the government. However, in the process of the co-firing power generation, the carbon emission parameters are mainly affected by the unit type, the coal combustion quality, and operating load. In this case, it is difficult to obtain the exact values about the carbon emission parameters. To overcome this difficulty, we will adopt the globalized robust counterpart constraint (5) to model this uncertainty:

$$\sum_{n=1}^{N}C_{mn}z_{mn}-x_m-y_m \leqslant \min_{\boldsymbol{C}'_m\in\mathcal{U}_1}\phi(\boldsymbol{C}_m,\boldsymbol{C}'_m), \quad \forall \boldsymbol{C}_m\in\mathcal{U}_2, m\in\mathcal{M}, \tag{5}$$

where the distance function $\phi(\boldsymbol{C}_m,\boldsymbol{C}'_m)=\alpha(\|\boldsymbol{C}_m-\boldsymbol{C}'_m\|_1)$ with $\alpha(t)=\theta t$, $t\geqslant 0$, $\theta\geqslant 0$ is the global sensitivity parameter.

**Remark 1.** If $\boldsymbol{C}_m\in\mathcal{U}_1$, then obviously $\min_{\boldsymbol{C}'_m\in\mathcal{U}_1}\phi(\boldsymbol{C}_m,\boldsymbol{C}'_m)=0$ holds, and constraint (5) simplifies into the uncertain constraint $\sum_{n=1}^{N}C_{mn}z_{mn}-x_m-y_m\leqslant 0$. That is to say, the GRO method requires full feasibility for all parameter values in the inner uncertainty set $\mathcal{U}_1$. However, for $\boldsymbol{C}_m\in\mathcal{U}_2\backslash\mathcal{U}_1$, the violation of uncertain constraint $\sum_{n=1}^{N}C_{mn}z_{mn}-x_m-y_m\leqslant 0$ is allowed, which is controlled by the distance $\min_{\boldsymbol{C}'_m\in\mathcal{U}_1}\phi(\boldsymbol{C}_m,\boldsymbol{C}'_m)$ of $\boldsymbol{C}_m$ to $\mathcal{U}_1$. In other words, infeasibilities are allowed for the parameter values in set $\mathcal{U}_2\backslash\mathcal{U}_1$, where the violation is controlled by the distance of the parameter value from the inner uncertainty set.

In addition, the value of the global sensitivity parameter $\theta$ directly affects the value of distance function $\phi(\boldsymbol{C}_m,\boldsymbol{C}'_m)$, while the value of the distance function $\phi(\boldsymbol{C}_m,\boldsymbol{C}'_m)$ reflects the degree to which uncertain constraint can be violated. If $\theta=0$, then $\phi=0$, that is, the uncertain constraint cannot be violated; if $\theta>0$, then the uncertain constraint can be violated to some extent. Therefore, the greater the $\theta$, the greater the degree to which the constraint can be violated, the larger the feasible domain of the BCC model, and the less conservative the government tax revenue objective.

**Demand constraints:** When the owners of the power plants make decisions, they have the obligation and responsibility to take into account the basic electricity demand of the society. This demand constraint is represented as,

$$\sum_{n=1}^{N}PC_{mn}(1-EC_m)z_{mn}-D_m\geqslant 0, \forall m\in\mathcal{M}. \tag{6}$$

**Fuel amount constraints:** In practice, each power plant has a different fuel storage capacity. In addition, the decision variable $z_{mn}$ should also satisfy the non-negative constraint. Thus, we have the following constraints:

$$0\leqslant z_{mn}\leqslant FA_{mn}, \forall m\in\mathcal{M}, n\in\mathcal{N}. \tag{7}$$

**Fuel quality constraints:** Because the chemical composition and the physical structure of the biomass fuel are different from those of the coal fuel, there are different equipment requirements in the co-firing process. If the mixed fuel cannot meet the requirements of the equipment, serious safety incidents will occur. To ensure the long-term sustainable production of power plants, their characteristics need to be constrained. The fuel quality is mainly considered in five aspects: volatile matter content, heat rate, ash content, moisture content, and sulfur content. In this case, the following constraints are required:

$$QB_{mq}^{L}\leqslant\frac{\sum_{n=1}^{N_a}F_{nq}z_{mn}}{\sum_{n=1}^{N_a}z_{mn}}\leqslant QB_{mq}^{U}, \forall m\in\mathcal{M}, q\in\mathcal{Q}, \tag{8}$$

$$QC_{mq}^{L}\leqslant\frac{\sum_{n=N_{a+1}}^{N}F_{nq}z_{mn}}{\sum_{n=N_{a+1}}^{N}z_{mn}}\leqslant QC_{mq}^{U}, \forall m\in\mathcal{M}, q\in\mathcal{Q}. \tag{9}$$

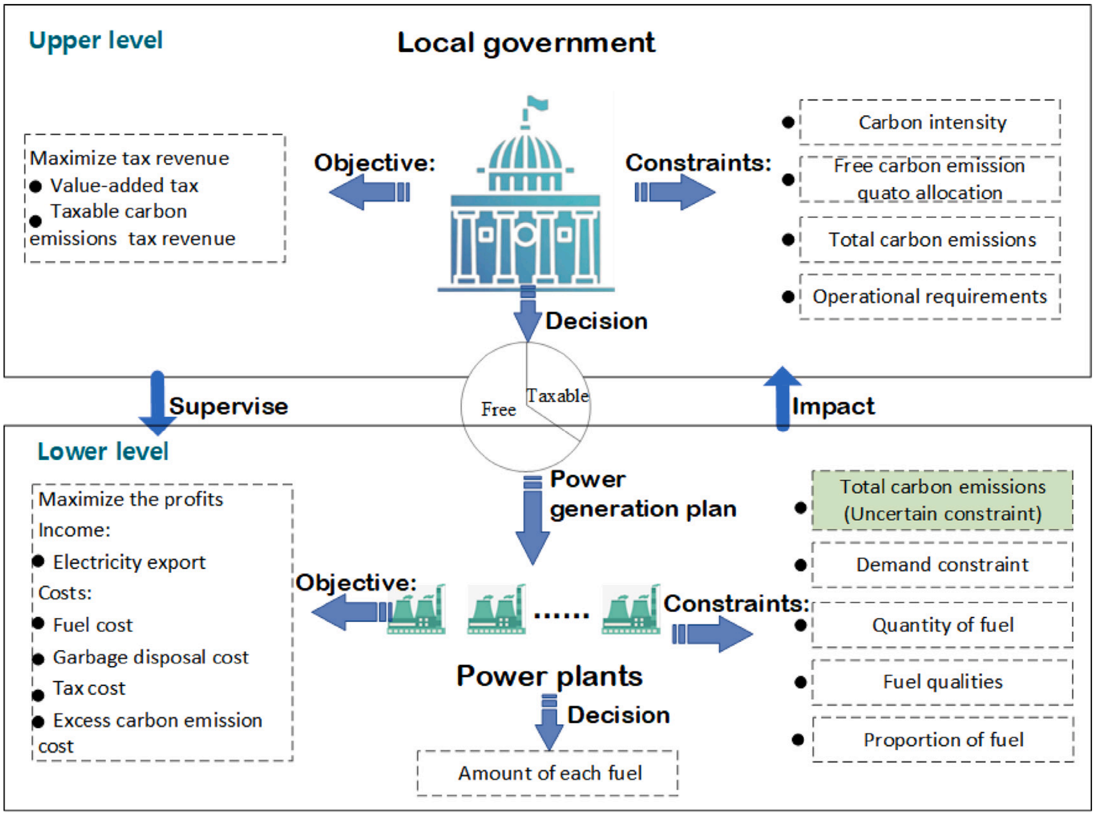


**Fig. 1.** Structure of the GRC bi-level BCC model.

**Proportion constraints:** The degree of burnout of the coal fuels is determined by the type of fuel and the proportion of biomass incorporated. In a coal-fired furnace, the BCC is easier to ignite than pure coal because of the high volatile content of the biomass. However, if the biomass–coal fuel combustion is insufficient, it will lead to the emission of the carbon-polluting gases such as the carbon monoxide and methane. Therefore, to ensure that the fuel is fully burned, the proportion of the biomass fuel needs to be controlled. Then the proportion of the biomass fuel is constrained as follows:

$$\frac{\sum_{n=1}^{N_a} z_{mn}}{\sum_{n=1}^{N} z_{mn}} \leqslant B_m, \forall m \in \mathcal{M}. \tag{10}$$

Finally, our model structure is shown in Fig. 1. The GRC bi-level BCC model is as follows:

**GRC bi-level BCC model**

$$\max \quad \mathrm{GTR} = \rho \sum_{m=1}^{M} \sum_{n=1}^{N} [PPC_{mn}(1 - EC_{mn}) - u_{mn} z_{mn}] + w \sum_{m=1}^{M} y_m$$

s.t. Constraints (1)–(4),

$$\begin{aligned} \max \quad \mathrm{PB}_m = P \sum_{n=1}^{N} PC_{mn}(1 - EC_{mn}) z_{mn} - \sum_{n=1}^{N} u_{mn} z_{mn} \\ - \sum_{n=1}^{N} \sum_{k=1}^{K} EP_{nk} TP_{nk} z_{mn} - \\ \rho \sum_{m=1}^{M} \sum_{n=1}^{N} [PPC_{mn}(1 - EC_{mn}) - u_{mn}] z_{mn} \\ - w \sum_{m=1}^{M} y_m - OC_m, \end{aligned} \tag{11}$$

s.t. Constraints (5)–(10).

It can be seen that the GRC bi-level BCC model can resist uncertainty. Nevertheless, Eq. (5) is a semi-infinite constraint, thus the solution of the bi-level model is difficult. In the next section, we will turn semi-infinite constraint (5) into a finite convex constraint system, then reformulate the bi-level model as a single-level mixed-integer programming model.

## 4. Main results about the GRC bi-level BCC model

This section is dedicated to obtaining the computationally tractable systems of the GRC bi-level BCC model. The main difficulties in solving the model lie in the following three aspects:

(1) The solution about the bi-level BCC problem is faced with a challenge, because (5) is a semi-infinite constraint, that is, the lower optimization model has a linear objective subject to infinite constraints.
(2) The existing studies show that the bi-level optimization problem is often difficult to solve. Therefore, even the semi-infinite constraint problem is turned in a finite system, our BCC bi-level optimization problem is still a difficult optimization problem.
(3) Since the complementary slackness constraints are formulated by the transformation from a bi-level model to a single-level model, the solution of our model is also confronted with nonlinear constraints.

To overcome the above difficulties, this section proceeds in three steps. First, we convert semi-infinite constraint (5) to a finite convex constraint system. Second, we convert the bi-level BCC model into a single-level model by using the KKT conditions. Third, we transform the nonlinear complementary tightness constraints into their equivalent linear constraints.

### 4.1. Reformation of the semi-infinite constraint

In this section, inner–outer uncertainty sets are discussed first, which can characterize the uncertain carbon emission parameters.

Then, semi-infinite constraint (5) is converted to a finite convex constraint system.

The uncertain carbon emission parameters $C_{mn}$ in constraint (5) vary in inner–outer uncertainty sets $(\mathcal{U}_1, \mathcal{U}_2)$ which are parameterized in the following affine form:

$$\mathcal{U}_1(\mathcal{U}_2) = \{\boldsymbol{C}_m = \boldsymbol{C}_m^0 + \sum_{l=1}^{L} \boldsymbol{C}_m^l \zeta^l | \zeta \in \mathcal{Z}_1(\mathcal{Z}_2)\},$$

where $\boldsymbol{C}_m^0$ is the nominal value, $\boldsymbol{C}_m^l$ is the basic shift, $\boldsymbol{\zeta} = [\zeta^1, \zeta^2, \dots, \zeta^L]$ is the perturbation vector and $\mathcal{Z}$ is the perturbation set.

According to the structure of uncertainty inner–outer sets $(\mathcal{U}_1, \mathcal{U}_2)$, the uncertainty sets are determined by the inner–outer perturbation sets $(\mathcal{Z}_1, \mathcal{Z}_2)$. The structure of the inner–outer perturbation sets $(\mathcal{Z}_1, \mathcal{Z}_2)$ will be given as,

$$\mathcal{Z}_1 = \{\boldsymbol{\zeta} \in R^L : \|\boldsymbol{\zeta}\|_\infty \leqslant 1, \|\boldsymbol{\zeta}\|_1 \leqslant \tau\}, 1 \leqslant \tau \leqslant L,$$

and

$$\mathcal{Z}_2 = \{\boldsymbol{\zeta} \in R^L : \|\boldsymbol{\zeta}\|_\infty \leqslant 1\}.$$

Based on the above uncertainty sets, the next step is to convert constraint (5) into a finite convex system. The equivalent form of semi-infinite constraint (5) is summarized in the following theorem.

**Theorem 1.** *Given a pair of uncertainty sets $(\mathcal{U}_1, \mathcal{U}_2)$, vector $\boldsymbol{z}_m \in R^N$ satisfies semi-infinite constraint (5) if and only if there exists $\boldsymbol{v}_m \in R^N$, $\boldsymbol{\Gamma}_m \in R^L$, $\boldsymbol{\eta}_m \in R^L$ such that the following finite convex constraints hold,*

$$(\boldsymbol{C}_m^0)^{\mathrm{T}} z_m + \|(\boldsymbol{A}_m^{\mathrm{T}})(\boldsymbol{z}_m - \boldsymbol{v}_m)\|_1 + \|\boldsymbol{\eta}_m\|_1 + \tau\|\boldsymbol{\Gamma}_m\|_\infty \leqslant x_m + y_m, \forall m \in \mathcal{M}, \tag{12a}$$

$$\boldsymbol{\eta}_m + \boldsymbol{\Gamma}_m = \boldsymbol{A}_m^{\mathrm{T}} \boldsymbol{v}_m, \forall m \in \mathcal{M}, \tag{12b}$$

$$\|\boldsymbol{v}_m\|_\infty \leqslant \theta, \forall m \in \mathcal{M}. \tag{12c}$$

*where $\boldsymbol{A}_m = [C_m^1, C_m^2, \dots, C_m^L]_{N\times L}$, and $\boldsymbol{z}_m = (z_{mn})_{n\in\mathcal{N}}$.*

**Proof.** The proof of Theorem 1 is in Appendix B. □

Theorem 1 converts semi-infinite constraint (5) into a finite convex constraint system. As a result, the GRC bi-level BCC model can be transformed into a deterministic bi-level BCC model.

### 4.2. Transforming bi-level BCC model into a single-level BCC model

Some constraints in the system (12) are nonlinear, which are not easy to handle. In the following, we linearize nonlinear constraints. By introducing the auxiliary variables $\xi_{m1}^l$, $\xi_{m2}^l$, $\xi_{m3}$ and $\xi_{m4}$, constraint system (12) is equivalent to the following linear system:

$$\sum_{n=1}^{N} C_{mn}^0 z_{mn} + \sum_{l=1}^{L} \xi_{m1}^l + \sum_{l=1}^{L} \xi_{m2}^l + \tau\xi_{m3} \leqslant x_m + y_m, \forall m \in \mathcal{M}, \tag{13a}$$

$$\xi_{m4} \leqslant \theta, \forall m \in \mathcal{M}, \tag{13b}$$

$$\eta_m^l + \Gamma_m^l = \sum_{n=1}^{N} C_{mn}^l v_{mn}, \forall m \in \mathcal{M}, \tag{13c}$$

$$-\xi_{m1}^l \leqslant \sum_{n=1}^{N} C_{mn}^l (z_{mn} - v_{mn}) \leqslant \xi_{m1}^l, \forall m \in \mathcal{M}, \tag{13d}$$

$$-\xi_{m2}^l \leqslant \eta_{m2}^l \leqslant \xi_{m2}^l, \forall m \in \mathcal{M}, \tag{13e}$$

$$-\xi_{m3} \leqslant \Gamma_m^l \leqslant \xi_{m3}, \forall m \in \mathcal{M}, \tag{13f}$$

$$-\xi_{m4} \leqslant v_{mn} \leqslant \xi_{m4}, \forall m \in \mathcal{M}. \tag{13g}$$

As a consequence, the GRC bi-level BCC model is equivalent to the following linear bi-level programming model,

$$\begin{aligned}
\max \quad & \mathrm{GTR} = \rho \sum_{m=1}^{M} \sum_{n=1}^{N} [PPC_{mn}(1 - EC_{mn}) - u_{mn} z_{mn}] + w \sum_{m=1}^{M} y_m \\
\text{s.t.} \quad & \text{Constraints (1)–(4)}, \\
& \max \quad \mathrm{PB}_m = P \sum_{n=1}^{N} PC_{mn}(1 - EC_{mn}) z_{mn} - \sum_{n=1}^{N} u_{mn} z_{mn} \\
& \qquad - \sum_{n=1}^{N} \sum_{k=1}^{K} EP_{nk} TP_{nk} z_{mn} - \\
& \qquad \rho \sum_{m=1}^{M} \sum_{n=1}^{N} [PPC_{mn}(1 - EC_{mn}) - u_{mn}] z_{mn} \\
& \qquad - w \sum_{m=1}^{M} y_m - OC_m, \\
& \text{s.t.} \quad \text{Constraints (6)–(10)} \quad \textit{and} \quad \text{(13a)–(13g)}.
\end{aligned}$$

This bi-level linear programming model establishes the connection between the upper level of the government and the lower level of the power plants. However, it is well-known that solving the bi-level model is a difficult task, the uncertain lower-level problem becomes even harder to solve. Some methods have been used to compute the bi-level model, one of which is the KKT method. Replacing the lower-level problem with its KKT condition, the bi-level model is then transformed into a single-level optimization problem (Sinha et al., 2017). The KKT conditions for the lower-level problem are stated in the following proposition.

**Proposition 1.** *The KKT conditions for the production planning of the lower-level power plants are composed of four aspects: Lagrangian stationarity, complementary slackness, dual feasibility, and primal feasibility. The four aspects are as follows,*
***Lagrangian stationarity:***

$$\begin{aligned}
& PPC_{mn}(1 - EC_{mn}) - u_{mn} - \sum_{k=1}^{K} EP_{nk} TP_{nk} - \rho[PPC_{mn}(1 - EC_{mn}) - u_{mn}] + \\
& PC_{mn}(1 - EC_{mn}) - \lambda_m^1 PC_{mn}(1 - EC_{mn}) - \lambda_m^8 (B_m - 1) + \lambda_m^9 C_{mn}^0 + \lambda_{ml}^{11} C_{mn}^l - \\
& \sum_{q=1}^{Q} \lambda_{mq}^5 (QB_{mq}^U - F_{nq}) - \sum_{q=1}^{Q} \lambda_{mq}^4 (QB_{mq} - F_{nq}) \\
& = 0, \forall m \in \mathcal{M}, \forall n \in \{1, \dots, N_a\}.
\end{aligned} \tag{14a}$$

$$\begin{aligned}
& PPC_{mn}(1 - EC_{mn}) - u_{mn} - \sum_{k=1}^{K} EP_{nk} TP_{nk} - \rho[PPC_{mn}(1 - EC_{mn}) - u_{mn}] + \\
& PC_{mn}(1 - EC_{mn}) - \lambda_m^1 PC_{mn}(1 - EC_{mn}) - \lambda_m^8 B_m + \lambda_m^9 C_{mn}^0 + \lambda_{ml}^{11} C_{mn}^l - \\
& \sum_{q=1}^{Q} \lambda_{mq}^7 (QB_{mq}^U - F_{nq}) - \sum_{q=1}^{Q} \lambda_{mq}^6 (QB_{mq} - F_{nq}) \\
& = 0, \forall m \in \mathcal{M}, \forall n \in \{N_{a+1}, \dots, N\}.
\end{aligned} \tag{14b}$$

***Complementary slackness:***

$$\lambda_m^1 (\sum_{n=1}^{N} PC_{mn}(1 - EC_m) z_{mn} - D_m) = 0, \tag{15a}$$

$$\lambda_{mn}^2 (z_{mn}) = 0, \tag{15b}$$

$$\lambda_{mn}^3 (FA_{mn} - z_{mn}) = 0, \tag{15c}$$

$$\lambda_{mq}^4 (\sum_{n=1}^{N_a} F_{nq} z_{mn} - QB_{mq}^L \sum_{n=1}^{N_a} z_{mn}) = 0, \tag{15d}$$

$$\lambda_{mq}^5 (QB_{mq}^U \sum_{n=1}^{N_a} z_{mn} - \sum_{n=1}^{N_a} F_{nq} z_{mn}) = 0, \tag{15e}$$

$$\lambda_{mq}^6 (\sum_{n=N_{a+1}}^{N} F_{nq} z_{mn} - QC_{mq}^L \sum_{n=N_{a+1}}^{N} z_{mn}) = 0, \tag{15f}$$

$$\lambda_{mq}^{7}(QC_{mq}^{U}\sum_{n=1}^{N_a} z_{mn} - \sum_{n=N_{a+1}}^{N} F_{nq} z_{mn}) = 0, \tag{15g}$$

$$\lambda_{m}^{8}(B_m \sum_{n=1}^{N} z_{mn} - \sum_{n=1}^{N_a} z_{mn}) = 0, \tag{15h}$$

$$\lambda_{m}^{9}(x_m + y_m - (\sum_{n=1}^{N} C_{mn}^{0} z_{mn} + \sum_{l=1}^{L} \xi_{m1}^{l} + \sum_{l=1}^{L} \xi_{m2}^{l} + \tau\xi_{m3})) = 0, \tag{15i}$$

$$\lambda_{m}^{10}(\theta - \xi_{m4}) = 0, \tag{15j}$$

$$\lambda_{ml}^{11}(\eta_m^l + \Gamma_m^l - \sum_{n=1}^{N} C_{mn}^{l} \upsilon_{mn}) = 0, \tag{15k}$$

$$\lambda_{ml}^{12}(\xi_{m1}^{l} + \sum_{n=1}^{N} C_{mn}^{l}(z_{mn} - \upsilon_{mn})) = 0, \tag{15l}$$

$$\lambda_{ml}^{13}(\xi_{m1}^{l} - \sum_{n=1}^{N} C_{mn}^{l}(z_{mn} - \upsilon_{mn})) = 0, \tag{15m}$$

$$\lambda_{ml}^{14}(\xi_{m2}^{l} + \eta_{m2}^{l}) = 0, \tag{15n}$$

$$\lambda_{ml}^{15}(\xi_{m2}^{l} - \eta_{m2}^{l}) = 0, \tag{15o}$$

$$\lambda_{ml}^{16}(\xi_{m3} - \Gamma_m^l) = 0, \tag{15p}$$

$$\lambda_{ml}^{17}(\xi_{m3} + \Gamma_m^l) = 0, \tag{15q}$$

$$\lambda_{m}^{18}(\xi_{m4} + \upsilon_{mn}) = 0, \tag{15r}$$

$$\lambda_{m}^{19}(\xi_{m4} - \upsilon_{mn}) = 0. \tag{15s}$$

***Dual feasibility:***

$$\lambda^i \geqslant 0, i \in \{1, \dots, 19\}. \tag{16}$$

***Primal feasibility:***

(6)–(10), (13a)–(13g). (17)

In light of Proposition 1, the following single-level model is obtained:

$$\begin{aligned} \max \quad & \mathrm{GTR} = \rho \sum_{m=1}^{M}\sum_{n=1}^{N}[PPC_{mn}(1-EC_{mn}) - u_{mn}]z_{mn} + w\sum_{m=1}^{M} y_m \\ \text{s.t.} \quad & \text{Constraints (1)–(4), (14)–(17).} \end{aligned} \tag{18}$$

Noting that constraints (15a)–(15s) in resulting single-level model (18) are nonlinear, thus they should be linearized, the results are stated in the following proposition.

**Proposition 2.** *By introducing auxiliary variables $\mu^i$ and a sufficiently large number M, the nonlinear complementary slackness constraints (15a)–(15s) are respectively equivalent to the following linear constraints,*

$$\begin{cases} \lambda_m^1 \leqslant M * \mu_m^1, \forall m \in \mathcal{M}, \\ \sum_{n=1}^{N} PC_{mn}(1-EC_m)z_{mn} - D_m \leqslant M*(1-\mu_m^1), \forall m \in \mathcal{M}. \end{cases} \tag{19a}$$

$$\begin{cases} \lambda_{mn}^2 \leqslant M * \mu_{mn}^2, \forall m \in \mathcal{M}, \forall n \in \mathcal{N}, \\ z_{mn} \leqslant M*(1-\mu_{mn}^2), \forall m \in \mathcal{M}, \forall n \in \mathcal{N}. \end{cases} \tag{19b}$$

$$\begin{cases} \lambda_{mn}^3 \leqslant M * \mu_{mn}^3, \forall m \in \mathcal{M}, \forall n \in \mathcal{N}, \\ FA_{mn} - z_{mn} \leqslant M*(1-\mu_{mn}^3), \forall m \in \mathcal{M}, \forall n \in \mathcal{N}. \end{cases} \tag{19c}$$

$$\begin{cases} \lambda_{mq}^4 \leqslant M * \mu_{mq}^4, \forall m \in \mathcal{M}, \forall q \in \mathcal{Q}, \\ \sum_{n=1}^{N_a} F_{nq}z_{mn} - QB_{mq}^{L}\sum_{n=1}^{N_a} z_{mn} \leqslant M*(1-\mu_{mq}^4), \forall m \in \mathcal{M}, \forall q \in \mathcal{Q}. \end{cases} \tag{19d}$$

$$\begin{cases} \lambda_{mq}^5 \leqslant M * \mu_{mq}^5, \forall m \in \mathcal{M}, \forall q \in \mathcal{Q}, \\ QB_{mq}^{U}\sum_{n=1}^{N_a} z_{mn} - \sum_{n=1}^{N_a} F_{nq}z_{mn} \leqslant M*(1-\mu_{mq}^5), \forall m \in \mathcal{M}, \forall q \in \mathcal{Q}. \end{cases} \tag{19e}$$

$$\begin{cases} \lambda_{mq}^6 \leqslant M * \mu_{mq}^6, \forall m \in \mathcal{M}, \forall q \in \mathcal{Q}, \\ \sum_{n=N_{a+1}}^{N} F_{nq}z_{mn} - QC_{mq}^{L}\sum_{n=N_{a+1}}^{N} z_{mn} \leqslant M*(1-\mu_{mq}^6), \forall m \in \mathcal{M}, \forall q \in \mathcal{Q}. \end{cases} \tag{19f}$$

$$\begin{cases} \lambda_{mq}^7 \leqslant M * \mu_{mq}^7, \forall m \in \mathcal{M}, \forall q \in \mathcal{Q}, \\ QC_{mq}^{U}\sum_{n=N_{a+1}}^{N} z_{mn} - \sum_{n=N_{a+1}}^{N} F_{nq}z_{mn} \leqslant M*(1-\mu_{mq}^7), \forall m \in \mathcal{M}, \forall q \in \mathcal{Q}. \end{cases} \tag{19g}$$

$$\begin{cases} \lambda_m^8 \leqslant M * \mu_m^8, \forall m \in \mathcal{M}, \\ B_m\sum_{n=1}^{N} z_{mn} - \sum_{n=1}^{N_a} z_{mn} \leqslant M*(1-\mu_m^8), \forall m \in \mathcal{M}. \end{cases} \tag{19h}$$

$$\begin{cases} \lambda_m^9 \leqslant M * \mu_m^9, \forall m \in \mathcal{M}, \\ x_m + y_m - (\sum_{n=1}^{N} C_{mn}^0 z_{mn} + \sum_{l=1}^{L}\xi_{m1}^l + \sum_{l=1}^{L}\xi_{m2}^l + \tau\xi_{m3}) \\ \quad \leqslant M*(1-\mu_m^9), \forall m \in \mathcal{M}. \end{cases} \tag{19i}$$

$$\begin{cases} \lambda_m^{10} \leqslant M * \mu_m^{10}, \forall m \in \mathcal{M}, \\ \theta - \xi_{m4} \leqslant M*(1-\mu_m^{10}), \forall m \in \mathcal{M}. \end{cases} \tag{19j}$$

$$\begin{cases} \lambda_{ml}^{11} \leqslant M * \mu_{ml}^{11}, \forall m \in \mathcal{M}, \forall l \in \mathcal{L}, \\ \eta_m^l + \Gamma_m^l - \sum_{n=1}^{N} C_{mn}^l \upsilon_{mn} \leqslant M*(1-\mu_{ml}^{11}), \forall m \in \mathcal{M}, \forall l \in \mathcal{L}. \end{cases} \tag{19k}$$

$$\begin{cases} \lambda_{ml}^{12} \leqslant M * \mu_{ml}^{12}, \forall m \in \mathcal{M}, \forall l \in \mathcal{L}, \\ \xi_{m1}^l + \sum_{n=1}^{N} C_{mn}^l(z_{mn}-\upsilon_{mn}) \leqslant M*(1-\mu_{ml}^{12}), \forall m \in \mathcal{M}, \forall l \in \mathcal{L}. \end{cases} \tag{19l}$$

$$\begin{cases} \lambda_{ml}^{13} \leqslant M * \mu_{ml}^{13}, \forall m \in \mathcal{M}, \forall l \in \mathcal{L}, \\ \xi_{m1}^l - \sum_{n=1}^{N} C_{mn}^l(z_{mn}-\upsilon_{mn}) \leqslant M*(1-\mu_{ml}^{13}), \forall m \in \mathcal{M}, \forall l \in \mathcal{L}. \end{cases} \tag{19m}$$

$$\begin{cases} \lambda_{ml}^{14} \leqslant M * \mu_{ml}^{14}, \forall m \in \mathcal{M}, \forall l \in \mathcal{L}, \\ \xi_{m2}^l + \eta_{m2}^l \leqslant M*(1-\mu_{ml}^{14}), \forall m \in \mathcal{M}, \forall l \in \mathcal{L}. \end{cases} \tag{19n}$$

$$\begin{cases} \lambda_{ml}^{15} \leqslant M * \mu_{ml}^{15}, \forall m \in \mathcal{M}, \forall l \in \mathcal{L}, \\ \xi_{m2}^l - \eta_{m2}^l \leqslant M*(1-\mu_{ml}^{15}), \forall m \in \mathcal{M}, \forall l \in \mathcal{L}. \end{cases} \tag{19o}$$

$$\begin{cases} \lambda_{ml}^{16} \leqslant M * \mu_{ml}^{16}, \forall m \in \mathcal{M}, \forall l \in \mathcal{L}, \\ \xi_{m3} - \Gamma_m^l \leqslant M*(1-\mu_{ml}^{16}), \forall m \in \mathcal{M}, \forall l \in \mathcal{L}. \end{cases} \tag{19p}$$

$$\begin{cases} \lambda_{ml}^{17} \leqslant M * \mu_{ml}^{17}, \forall m \in \mathcal{M}, \forall l \in \mathcal{L}, \\ \xi_{m3} + \Gamma_m^l \leqslant M*(1-\mu_{ml}^{17}), \forall m \in \mathcal{M}, \forall l \in \mathcal{L}. \end{cases} \tag{19q}$$

$$\begin{cases} \lambda_m^{18} \leqslant M * \mu_m^{18}, \forall m \in \mathcal{M}, \\ \xi_{m4} + \upsilon_{mn} \leqslant M*(1-\mu_m^{18}), \forall m \in \mathcal{M}. \end{cases} \tag{19r}$$

$$\begin{cases} \lambda_m^{19} \leqslant M * \mu_m^{19}, \forall m \in \mathcal{M}, \\ \xi_{m4} - \upsilon_{mn} \leqslant M*(1-\mu_m^{19}), \forall m \in \mathcal{M}. \end{cases} \tag{19s}$$

Finally, the overall structure of the computationally tractable process is shown in Fig. 2. The computationally tractable system of GRC bi-level BCC model (11) is reformulated as follows,

$$\begin{aligned} \max \quad & \mathrm{GTR} = \rho \sum_{m=1}^{M}\sum_{n=1}^{N}[PPC_{mn}(1-EC_{mn}) - u_{mn}]z_{mn} + w\sum_{m=1}^{M} y_m \\ \text{s.t.} \quad & \mu_i \in \{0,1\}, \quad i \in \{1,\dots,19\}, \\ & \text{Constraints (1)–(4), (6)–(10),} \\ & \text{(14), (16)–(17), (19).} \end{aligned} \tag{20}$$

In summary, semi-infinite constraint (5) is first transformed into a finite convex constraint system, then the lower-level power plant

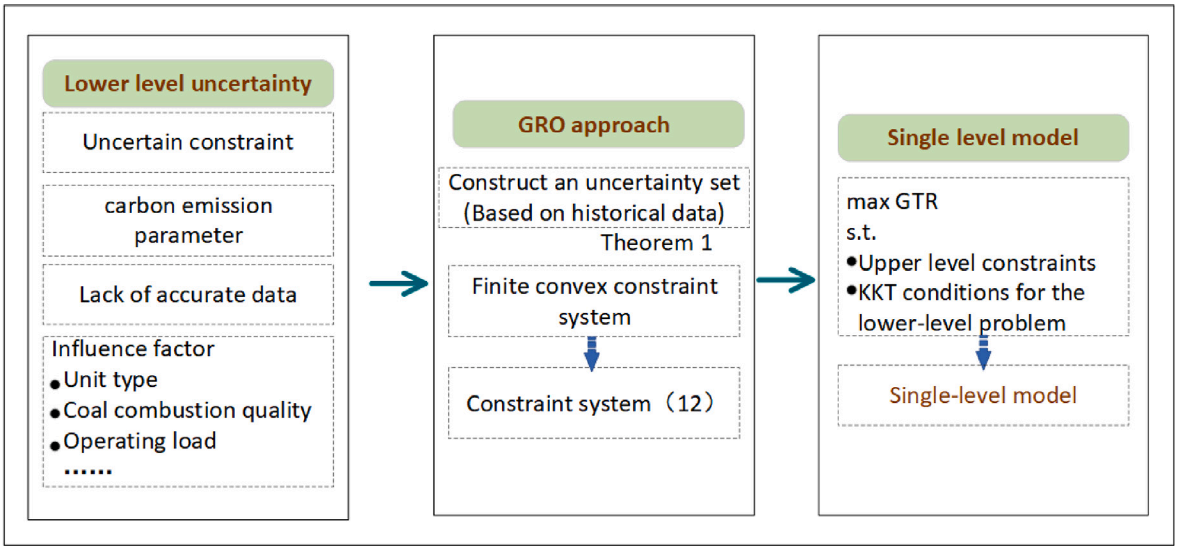


**Fig. 2.** The transformation of GRC bi-level BCC model into a single-level deterministic model.

**Table 2**
Fuel quality requirements.

| Fuel | Quality | Linyi | | Shiliquan | | Shanxian | |
|---|---|---|---|---|---|---|---|
| | | Lower bound | Upper bound | Lower bound | Upper bound | Lower bound | Upper bound |
| Coal | Volatile matter (%) | 8.53 | 43.49 | 9.31 | 34.9 | 9.01 | 40.7 |
| | Heat rate (GJ/tonne) | 20.19 | | 16.57 | | 18.67 | |
| | Ash content (%) | | 26.3 | | 25.2 | | 28.9 |
| | Moisture content (%) | | 11.3 | | 12.6 | | 10.7 |
| | Sulfur content (%) | | 0.63 | | 0.59 | | 0.58 |
| Biomass | Volatile matter (%) | 22.13 | 73.21 | 20.15 | 69.47 | 21.77 | 75.42 |
| | Ash content (%) | | 13.65 | | 12.71 | | 12.96 |
| | Moisture content (%) | | 12.07 | | 10.57 | | 10.21 |

**Table 3**
Parameters for each power plant.

| Parameters | Power plants | | |
|---|---|---|---|
| | Linyi | Shiliquan | Shanxian |
| Operating costs ($10^8$ CNY) | 1.61 | 0.82 | 1.31 |
| Minimum allocation quotas ($10^6$ tonnes) | 2.38 | 0.97 | 2.29 |
| Maximum allocation quotas ($10^6$ tonnes) | 8.21 | 4.93 | 5.34 |
| Electricity consumption rates (%) | 9.4 | 8.7 | 10.4 |
| Upper biomass proportions (%) | 27 | 29 | 27 |

production planning problem is replaced with its KKT conditions. After that, the complementary slackness conditions are linearized. As a consequence, our GRC bi-level BCC model (11) can be transformed into a computationally tractable single-level model (20), which can be computed efficiently by commercial optimization solver.

## 5. Method implementation in a real case

We address a real case about the power plants in Shandong Province China. In this section, to illustrate the validity and practicality of our optimization method, the numerical experiment consists of the following four parts. First, the computational results of our GRC bi-level BCC model are reported. Second, the validity of the proposed model is shown by comparing it with the nominal model and the RC model. Third, a sensitivity analysis about the global sensitivity parameter $\theta$, and the size of the inner uncertainty set is performed. Finally, several management insights are offered to managers. All numerical experiments are solved by CPLEX(12.8.0) on a personal computer.

### 5.1. Case description and data source

On 22 September 2020, China set out a dual carbon goal, aiming to peak its carbon dioxide emissions by 2030 and achieve carbon neutrality by 2060. According to these goals, the power sector's carbon emissions need to be given some attention. Based on statistics, approximately 45% of China's $CO_2$ emissions come from the power sector. In the important stage of the sustainable development, reducing the carbon emissions of the power industry is important, and finding a balance between the economy and the carbon emissions is also important.

Over the past years, overreliance on the fossil fuels has led to a significant reduction in the number of the fossil fuels. Meanwhile, the burning of the fossil fuels has created serious environmental problems. For the sake of sustainability, industries are looking for alternatives to coal to alleviate the shortage of non-renewable energy. In addition, due to the impact of COVID-19, the economic recovery is facing serious challenges. Based on the situation described above, the power plants need to change their paths to achieve a sustainable transformation. In the power sector, the BCC for power generation will not only reduce the amount of coal used but also reduce the carbon emissions.

As a large agricultural province, Shandong has an abundance of the agricultural waste such as peanut shells, corn straw, wheat straw, and cotton straw. This not only provides the biomass fuel for the BCC power generation but also increases the income of the local farmers (Li et al., 2023). In this case study, three BCC power plants using wood waste, straw, and coal in Shandong Province are selected in our case: Shanxian Power Plant, Shiliquan Power Plant, and Linyi Power Plant; the locations are presented in Fig. 3. The Shandong Province Government determines the CEQA to the power plants based on the

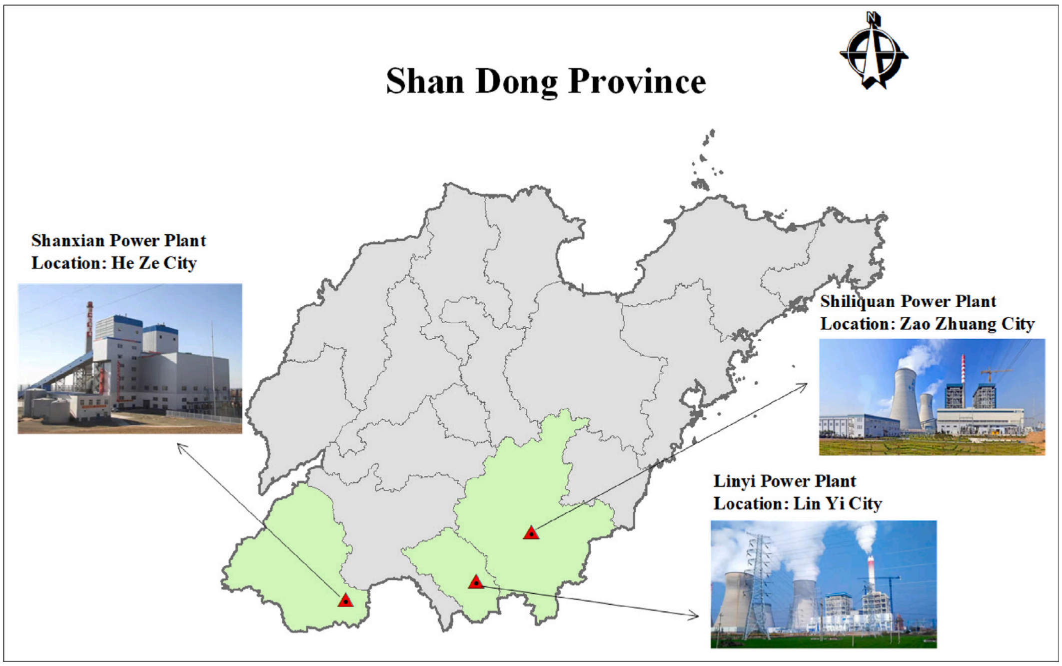


**Fig. 3.** Locations of the power plants.

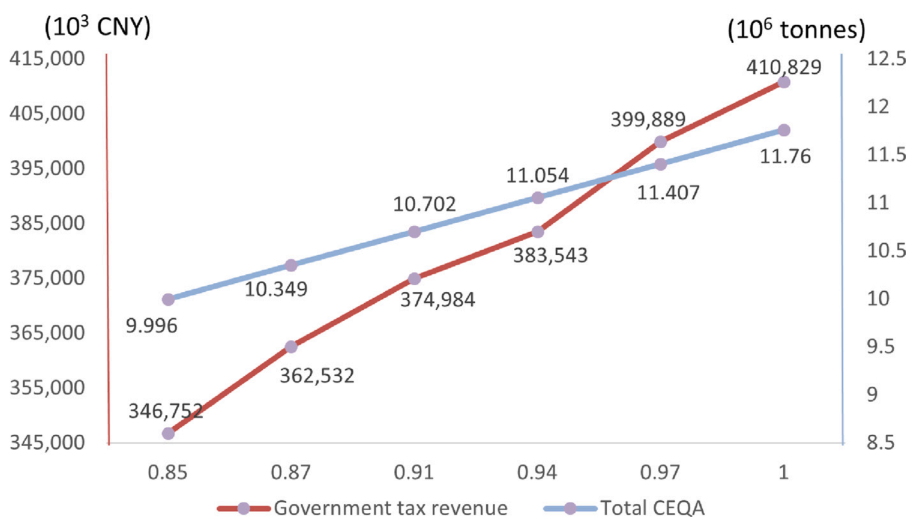


**Fig. 4.** Government tax revenue and total CEQA under different $\beta$.

local socioeconomic conditions. The power plant then formulates its production plan based on the CEQA set by the government to achieve the objective of maximizing profits.

The data used in our case and its source are given below. First, the upper and lower bound requirements for the volatile matter and heat rate of the coal fuel and biomass fuel for each power plant are given in Table 2. Other parameters related to the power plants are given in Tables 3 and 4. Second, the volatile matter and the heat rate of the biomass fuel and coal fuel are obtained from paper (Nussbaumer, 2003), and the data are presented in Table 5. For example, the fuel prices and pollution treatment costs in Table 6 are derived from the website of the Ministry of Ecology and Environment of the Peoples Republic of China. Finally, according to the Chinese National Development and Reform Commission, the electric power price is 0.45 CNY/kWh, the value-added tax rate is 0.17, and the excess carbon emission tax rate is 22.704 CNY/tonne. From Shandong Provinces 2021 Statistical Yearbook, the total basic power demand of Linyi City, Shiliquan City and Shanxian City is $4.98 \times 10^{10}$ kWh, $1.73 \times 10^{10}$ kWh and $2.56 \times 10^{10}$ kWh. In this case, 10% of the total basic power demand is selected. The total CEQA is $12.56 \times 10^6$ tonnes. In addition, for uncertain carbon emission parameters, the basic shift $C^l_{mn}$ is assumed to be 0.5% of the nominal value. In the following numerical experiment, $\mathbb{K}$ represents $10^5$.

### 5.2. Computational results

In this section, to demonstrate the effectiveness of the proposed GRC bi-level BCC model, the results are presented in two cases. In Case 1, the parameters are set as: $\mu = 0.8$, $r = 0.78$, and $\beta$ is changing from 0.85 to 1. In Case 2, the parameters are set as: $\mu = 0.8$, $\beta = 0.92$, and

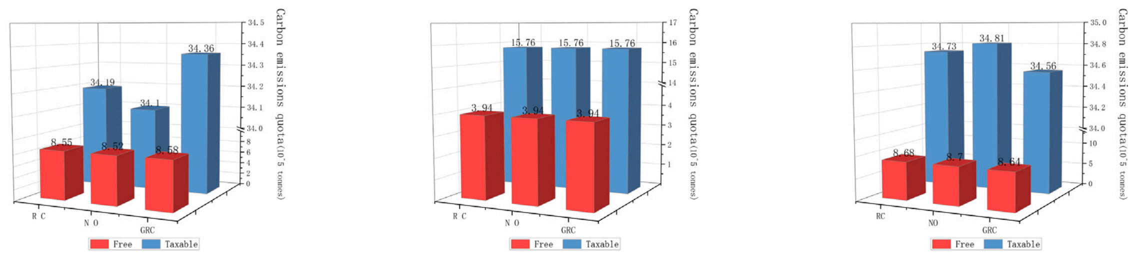


(a) Linyi (b) Shiliquan (c) Shanxian

**Fig. 5.** Carbon emissions quota allocation for each power plant.

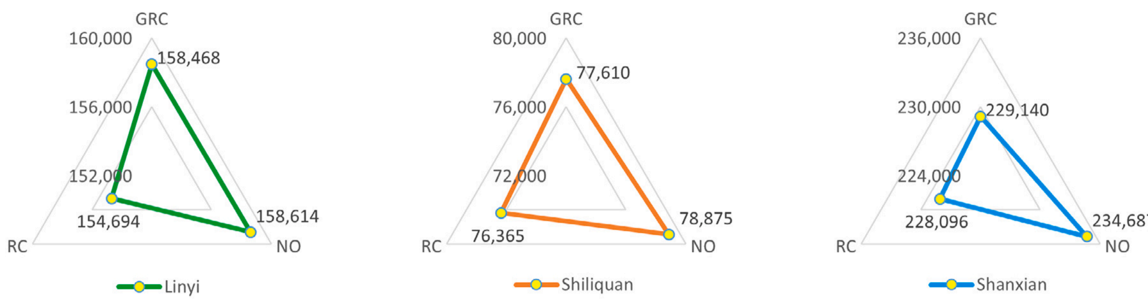


(a) Linyi ($10^3$ CNY) (b) Shiliquan ($10^3$ CNY) (c) Shanxian ($10^3$ CNY)

**Fig. 6.** Profit of each power plant under different models.

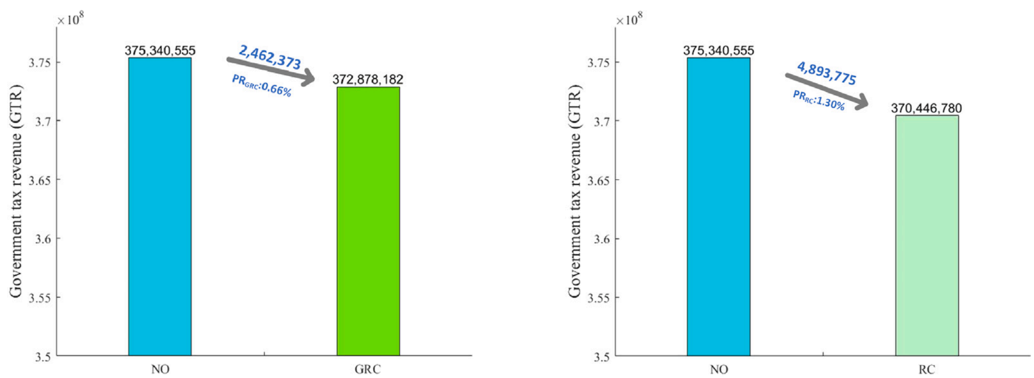


(a) GRC VS NO (b) RC VS NO

**Fig. 7.** Comparison of government tax revenue under different models.

**Table 4**
Parameters for each power plant.

| | Power conversion (kWh/ton) | | | | Carbon emissions (kg/ton) | |
|---|---|---|---|---|---|---|
| | Straw | Wood | Coal 1 | Coal 2 | Coal 1 | Coal 2 |
| Linyi | 1610 | 1780 | 2380 | 2490 | 2420 | 2230 |
| Shiliquan | 1600 | 1670 | 2400 | 2240 | 2530 | 2240 |
| Shanxian | 1510 | 1720 | 2470 | 2460 | 2460 | 2310 |

$r$ is changing from 0.77 to 0.82. In both cases, the parameters related to the inner–outer uncertainty sets are set as: $\theta = 1.2\ \mathbb{K}$, $\rho = 1.5$. The results report the government decisions and the production planning of the power plants in two cases.

Table 7 presents the government decisions and the power plant production plans under Case 1. We first analyze the government decisions. Table 7 shows that as the carbon emission control parameter $\beta$ increases from 0.85 to 1, the government tax revenue sharply increases from 346,753 $\times$ $10^3$ CNY to 410,829 $\times$ $10^3$ CNY. In terms of the carbon emission quota allocation, we find that both the free and the taxable carbon emission quota allocation of the power plants in Linyi and Shanxian show a downward trend. For instance, the free CEQA for the Shanxian power plant increases from 3.051 $\times$ $10^5$ tonnes to 4.272 $\times$ $10^5$ tonnes, and the taxable CEQA increases from 0.763 $\times$ $10^5$ tonnes to 1.068 $\times$ $10^5$ tonnes. In addition, there are no changes in the carbon emission quota allocated to the Shiliquan power plant.

We next analyze the production plans of the three power plants. From the surface data in Table 7, as parameter $\beta$ increases from 0.85 to 1, the profit of the Linyi power plant increases initially, followed by a decrease, but then again increases. However, the profit of the Shanxian power plant sharply increases. With a 15% increase in the

**Table 5**
Parameters for each fule.

| | | Straw | Wood waste | Coal 1 | Coal 2 |
|---|---|---|---|---|---|
| Fuel properties | Volatile matter (% weight) | 60.72 | 69.96 | 24.69 | 34.32 |
| | Heat rate (GJ/tonne) | 19.50 | 20.10 | 23.61 | 30.11 |
| | Ash content (% weight) | 12.20 | 8.90 | 11.21 | 9.67 |
| | Moisture content (% weight) | 6.01 | 12.70 | 7.70 | 5.60 |
| | Sulfur content (% weight) | 0.21 | 0.14 | 0.63 | 0.36 |
| Pollutant emissions | $SO_2$ (kg/ton) | 4.14 | 2.11 | 4.71 | 4.81 |
| | $NO_x$ (kg/ton) | 4.32 | 1.27 | 8.96 | 7.97 |

**Table 6**
Price parameters.

| | Price of fuel (CNY/ton) | | | | Pollutions cost (CNY/ton) | |
|---|---|---|---|---|---|---|
| | Straw | Wood | Coal 1 | Coal 2 | $SO_2$ | $NO_x$ |
| Linyi | 743 | 781 | 621 | 678 | 2.31 | 14.96 |
| Shiliquan | 727 | 828 | 602 | 678 | 1.92 | 14.43 |
| Shanxian | 731 | 771 | 562 | 682 | 2.14 | 14.81 |

carbon emission control parameter, the profit of the Shanxian power plant increases by 49%. In addition, under different carbon emission control parameters $\beta$, the fuel consumption of the power plants varies significantly. For example, when $\beta$ changes from 0.97 to 0.94, the wood fuel in the Shanxian power plant directly changes from $4.82 \times 10^5$ tonnes to 0. This also means that the power plants need to develop corresponding production plans based on different carbon emission control parameters $\beta$.

Table 8 shows the computational results under different value of parameter TEC with fixed parameter $\beta = 0.9$. From this result, we find that with the increase of parameter TEC, the government tax revenue also increases. Therefore, in addition to the carbon emission control parameter $\beta$, the parameter TEC also has a positive impact on the government tax revenue.

Therefore, both the carbon emission control parameter $\beta$ and parameter TEC have positive impacts on the government tax revenue.

Table 9 presents the government decisions and production plans for the power plants in Case 2. For government decisions, as $r$ increases from 0.77 to 0.82, the government tax revenue first rises to $379{,}135 \times 10^3$ CNY and then remains steady. For the carbon emission allowances, when $r$ grows from 0.77 to 0.82, the carbon emission quota allocation for the Linyi power plant and Shanxian power plant also shows a trend of rising first and then remaining steady. Only when $r$ is 0.77 does the carbon emission quota allocated to the Shiliquan power plant change.

From Table 9, it can be concluded that different carbon intensity control parameters $r$ also have an impact on the fuel consumption of the power plants. For example, when $r$ changes from 0.8 to 0.78, the coal 2 fuel consumption of the Linyi power plant changes from 0 to $2.581 \times 10^5$ tonnes. This indicates that when parameter $r$ changes, the production plan of the power plant also needs to be adjusted accordingly. Under different values of parameter $r$, the profit of each power plant also varies.

In addition to the tax economy, this section also analyzes the total carbon emission quota to obtain the environmental impact. From Fig. 4, it can be seen that with the relaxation of the carbon emission constraints, both the government tax revenue and the total CEQA increase. When the carbon emission control parameter $\beta$ takes values 0.85, 0.88, 0.91, 0.94, 0.97, and 1, the government tax revenue will increase by $15,779 \times 10^3$ CNY, $12,452 \times 10^3$ CNY, $8,559 \times 10^3$ CNY, $16,346 \times 10^3$ CNY, and $10,949 \times 10^3$, respectively.

In summary, the computational results in Case 1 and Case 2 could provide advice for the government to set the carbon emission quota allocations and the power plants to develop production plans.

### 5.3. Comparative studies

The following comparative analysis is divided into two parts. First, the solutions of the GRC bi-level BCC model (GRC) and the nominal bi-level BCC model (NO) are compared. Second, we compare the GRC bi-level BCC model with the robust bi-level BCC model (RC) in terms of conservatism. In the NO model, the carbon emission parameter is deterministic and assumed to be its nominal value. In the RC model, the uncertain carbon emission parameter varies within the outer uncertainty set $\mathcal{U}_2$, which means that the solution is completely feasible for the uncertainty set $\mathcal{U}_2$. The adjustable parameter settings in this section are: $\mu = 0.8$, $r = 0.78$, $\beta = 0.9$, $\theta = 10\ \mathbb{K}$, and $\rho = 1.5$.

#### 5.3.1. Comparison of the solutions obtained from different models

The carbon emission quota allocation decisions for three models are shown in Fig. 5. For example, in Fig. 5, sub Fig. 5(c) shows that the free carbon emission quota allocation decided by the government for the Shiliquan power plant under the GRC model, RC model and NO model are $34.19 \times 10^5$ tonnes, $34.10 \times 10^5$ tonnes, $34.36 \times 10^5$ tonnes respectively. The taxable carbon emission quota allocations under the three different optimization models are $8.55 \times 10^5$ tonnes, $8.52 \times 10^5$ tonnes, and $8.58 \times 10^5$ tonnes.

In addition, the production plans of the three power plants are presented in Table 10. For instance, the amount of straw consumed by the Shiliquan power plant is $1.117 \times 10^5$ tonnes, $1.125 \times 10^5$ tonnes and $1.108 \times 10^5$ tonnes under the GRC model, RC model and NO model, respectively. Fig. 6 shows the profit of three power plants, and it can be observed that compared to the NO model, the profit of each power plant under the GRC model and RC model has changed. For example, from the Fig. 6(a), the profit of the Linyi Power Plant is $158{,}614 \times 10^3$ CNY under the NO model, while under the GRC and RC models, the profit of the Linyi Power Plant is $158{,}468 \times 10^3$ CNY and $154{,}694 \times 10^3$ CNY, respectively.

It can be observed that compared to the NO model with fixed carbon emission parameter, the carbon emission quota allocation of the uncertain RC model and GRC model have completely changed. That is, when the determined value of carbon emission parameter cannot be obtained, the solution of the NO model is no longer the optimal solution, and even the solution is no longer a feasible solution. Therefore, the uncertainty of carbon emission parameter poses a challenge to the stability of the NO model. Unlike the NO model, the GRC and RC models can effectively resist the impact of uncertain carbon emission parameters. However, the conservatism of government tax revenue in the GRC and RC models still needs further analysis.

#### 5.3.2. Comparing the conservatism about different models

To further illustrate the superiority of our GRC model, this section provides a comparison about the robustness price of the GRC and RC models.

As mentioned above, the GRC model and RC model can effectively resist the influence of uncertain parameters. However, Fig. 7 shows that the government tax revenue in the NO model is larger than that in the GRC model and RC model. The part where the government tax revenue in the GRC and RC models are lower than those in the NO model is a

**Table 7**
Computational results under different value of $\beta$.

| $\beta$ | Government tax revenue | CEQA | Power plant | Profit | Free CEQA | Taxable CEQA | Fules | | | |
|---|---|---|---|---|---|---|---|---|---|---|
| | | | | | | | Straw | Wood | Coal 1 | Coal 2 |
| | ($10^3$ CNY) | ($10^6$ tonnes) | | ($10^3$ CNY) | ($10^6$ tonnes) | ($10^6$ tonnes) | ($10^5$ tonnes) | ($10^5$ tonnes) | ($10^5$ tonnes) | ($10^5$ tonnes) |
| 1 | 410,829 | 11.760 | Linyi | 169,427 | 3.560 | 0.890 | 0.806 | 6.105 | 12.971 | 5.715 |
| | | | Shiliquan | 58,945 | 1.576 | 0.394 | 3.442 | 0.000 | 7.178 | 1.248 |
| | | | Shanxian | 311,126 | 4.272 | 1.068 | 3.014 | 4.975 | 17.600 | 4.000 |
| 0.97 | 399,889 | 11.407 | Linyi | 154,174 | 3.409 | 0.852 | 0.765 | 5.793 | 14.328 | 3.406 |
| | | | Shiliquan | 76,713 | 1.576 | 0.394 | 1.111 | 2.331 | 7.178 | 1.248 |
| | | | Shanxian | 297,570 | 4.140 | 1.035 | 2.921 | 4.822 | 17.061 | 3.877 |
| 0.94 | 383,543 | 11.054 | Linyi | 148,081 | 3.337 | 0.834 | 0.765 | 5.799 | 9.363 | 8.386 |
| | | | Shiliquan | 58,945 | 1.576 | 0.394 | 3.442 | 0.000 | 7.178 | 1.248 |
| | | | Shanxian | 270,772 | 3.930 | 0.982 | 7.351 | 0.000 | 16.194 | 3.681 |
| 0.91 | 374,984 | 10.702 | Linyi | 155,384 | 3.423 | 0.855 | 0.765 | 5.793 | 15.314 | 2.416 |
| | | | Shiliquan | 76,713 | 1.576 | 0.394 | 1.111 | 2.331 | 7.178 | 1.248 |
| | | | Shanxian | 237,725 | 3.562 | 0.890 | 2.513 | 4.149 | 14.678 | 3.336 |
| 0.88 | 362,532 | 10.349 | Linyi | 155,990 | 3.430 | 0.858 | 0.765 | 5.792 | 15.807 | 1.922 |
| | | | Shiliquan | 76,713 | 1.576 | 0.394 | 1.111 | 2.331 | 7.178 | 1.248 |
| | | | Shanxian | 207,803 | 3.273 | 0.818 | 2.309 | 3.812 | 13.487 | 3.065 |
| 0.85 | 346,753 | 9.996 | Linyi | 150.842 | 3.369 | 0.842 | 0.766 | 5.797 | 11.613 | 6.129 |
| | | | Shiliquan | 58.945 | 1.576 | 0.394 | 3.442 | 0.000 | 7.178 | 1.248 |
| | | | Shanxian | 157.684 | 3.051 | 0.763 | 5.708 | 0.000 | 12.575 | 2.858 |

**Table 8**
Computational results under different value of parameter TEC.

| TEC | Government tax revenue | CEQA | Power plant | Profit | Free CEQA | Taxable CEQA | Fules | | | |
|---|---|---|---|---|---|---|---|---|---|---|
| | | | | | | | Straw | Wood | Coal 1 | Coal 2 |
| $10^6$ (tonnes) | ($10^3$ CNY) | ($10^6$ tonnes) | | ($10^3$ CNY) | ($10^6$ tonnes) | ($10^6$ tonnes) | ($10^5$ tonnes) | ($10^5$ tonnes) | ($10^5$ tonnes) | ($10^5$ tonnes) |
| 11 | 343,415 | 9.900 | Linyi | 155,988 | 3.430 | 0.857 | 0.765 | 5.792 | 15.806 | 1.923 |
| | | | Shiliquan | 76,713 | 1.576 | 0.394 | 1.110 | 2.331 | 7.178 | 1.248 |
| | | | Shanxian | 207,904 | 2.971 | 0.742 | 5.558 | 0.000 | 12.246 | 2.783 |
| 11.5 | 362,574 | 1.035 | Linyi | 151,092 | 3.372 | 0.843 | 0.765 | 5.796 | 11.817 | 5.924 |
| | | | Shiliquan | 58,945 | 1.576 | 0.394 | 3.442 | 0.000 | 7.178 | 1.248 |
| | | | Shanxian | 150,147 | 3.273 | 0.818 | 2.310 | 3.813 | 13.491 | 3.066 |
| 12 | 378,458 | 1.080 | Linyi | 155,216 | 3.421 | 0.855 | 0.765 | 5.793 | 15.177 | 2.554 |
| | | | Shiliquan | 76,713 | 1.576 | 0.394 | 1.110 | 2.331 | 7.178 | 1.248 |
| | | | Shanxian | 246,071 | 3.642 | 0.910 | 2.570 | 4.243 | 15.010 | 3.411 |
| 12.5 | 390,342 | 1.125 | Linyi | 147,571 | 3.331 | 0.832 | 0.765 | 5.799 | 8.948 | 8.803 |
| | | | Shiliquan | 58,945 | 1.576 | 0.394 | 3.442 | 0.000 | 7.178 | 1.248 |
| | | | Shanxian | 256,127 | 4.092 | 1.023 | 7.654 | 0.000 | 16.863 | 3.832 |
| 13 | 390,342 | 1.170 | Linyi | 164,715 | 3.512 | 0.878 | 0.795 | 6.023 | 12.753 | 5.684 |
| | | | Shiliquan | 58,945 | 1.576 | 0.394 | 3.442 | 0.000 | 7.178 | 1.248 |
| | | | Shanxian | 311,126 | 4.272 | 1.068 | 3.0144 | 4.975 | 17.600 | 4.000 |
| 13.5 | 426,056 | 1.215 | Linyi | 155,679 | 3.426 | 0.856 | 0.765 | 5.792 | 15.554 | 2.175 |
| | | | Shiliquan | 121,471 | 2.021 | 0.505 | 1.424 | 2.988 | 9.202 | 1.600 |
| | | | Shanxian | 311,126 | 4.272 | 1.068 | 3.0144 | 4.975 | 17.600 | 4.000 |

price paid to resist uncertainty. The robustness price of the GRC (RC) model is defined as follows:

$$\mathrm{PR}_{\mathrm{GRC}} = \frac{\mathrm{NO}^* - \mathrm{GRC}^*}{\mathrm{NO}^*} \times 100\%,$$

$$\mathrm{PR}_{\mathrm{RC}} = \frac{\mathrm{NO}^* - \mathrm{RC}^*}{\mathrm{NO}^*} \times 100\%,$$

where $(\cdot)^*$ represents the optimal government tax revenue.

Fig. 7 demonstrates that the government tax revenues under the GRC model, RC model and NO model are 372,878,182 CNY, 370,446, 780 CNY and 375,340,555 CNY, respectively. The robustness price of the GRC model and the RC model are 0.66% and 1.30%, respectively. Besides, compared with the RC model, the government tax revenue of the GRC model is $2,431,402$ CNY more, and the robustness price is 0.64% less.

This illustrates that, compared with the RC model, the GRC model pays a lower price to immunize against the effect of uncertain carbon emission parameters. Consequently, the government tax revenue objective in the RC model is more conservative than in the GRC model. In terms of the price of resisting uncertainty, the GRO method applied in this paper has advantages over the RO method. In short, the GRC model can not only resist the influence of uncertain parameters, but also be less conservative.

### 5.4. Sensitivity analysis

In this section, we analyze the influence of the global sensitivity parameter $\theta$ and the parameter $\tau$ on government tax revenue, and profit of each power plant in the GRC bi-level BCC model. The adjustable parameter settings in this section are: $\mu = 0.8$, $r = 0.78$, and $\beta = 0.9$. This set of adjustable parameters is selected from their reasonable ranges. In addition, we have explored the other two sets of sensitivity analysis in Appendix C.

#### 5.4.1. The effects of parameter $\theta$

In this section, the changes in government tax revenue and profit of each power plant under different global sensitivity parameters $\theta$ are analyzed.

The government tax revenue objective is given in Fig. 8. When the global sensitivity parameter $\theta$ increases from $5\mathbb{K}$ to $12\mathbb{K}$, the

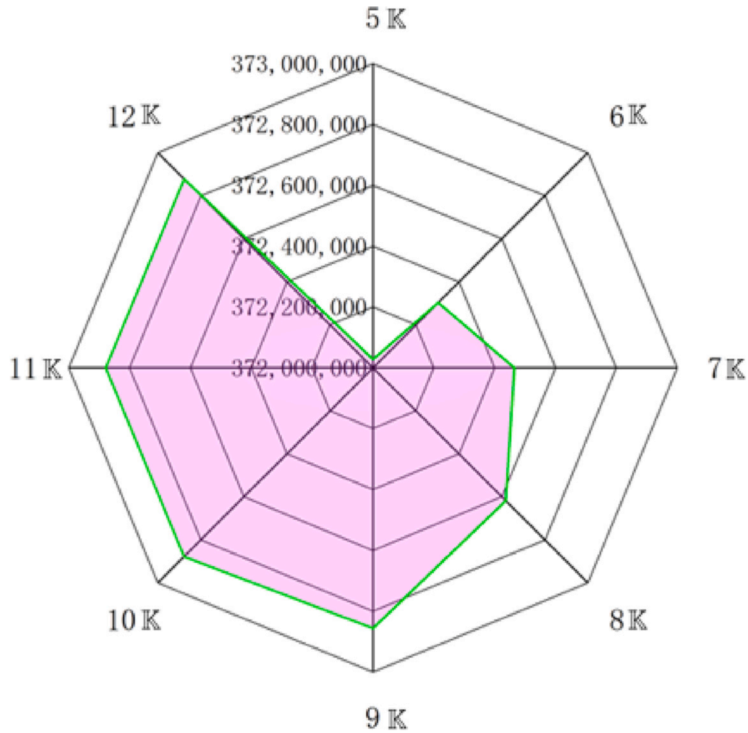


**Fig. 8.** The government tax revenue under different $\theta$.

**Table 9**
Computational results under different value of $r$.

| r | Government tax revenue ($10^3$ CNY) | CEQA ($10^6$ tonnes) | Power plant | Profit ($10^3$ CNY) | Free CEQA ($10^6$ tonnes) | Taxable CEQA ($10^6$ tonnes) | Fules Straw ($10^5$ tonnes) | Wood ($10^5$ tonnes) | Coal 1 ($10^5$ tonnes) | Coal 2 ($10^5$ tonnes) |
|---|---|---|---|---|---|---|---|---|---|---|
| 0.82 | 379,140 | 10.819 | Linyi | 158,341 | 3.459 | 0.864 | 0.765 | 5.790 | 17.723 | 0.000 |
| | | | Shiliquan | 76,713 | 1.576 | 0.394 | 1.111 | 2.331 | 7.178 | 1.248 |
| | | | Shanxian | 243,854 | 3.621 | 0.905 | 2.556 | 4.218 | 14.922 | 3.391 |
| 0.81 | 379,140 | 10.819 | Linyi | 158,341 | 3.459 | 0.864 | 0.765 | 5.790 | 17.723 | 0.000 |
| | | | Shiliquan | 76,713 | 1.576 | 0.394 | 1.111 | 2.331 | 7.178 | 1.248 |
| | | | Shanxian | 243,854 | 3.621 | 0.905 | 2.556 | 4.218 | 14.922 | 3.391 |
| 0.8 | 379,141 | 10.819 | Linyi | 158,341 | 3.458 | 0.864 | 0.765 | 5.790 | 17.723 | 0.000 |
| | | | Shiliquan | 76,713 | 1.576 | 0.394 | 1.111 | 2.331 | 7.178 | 1.248 |
| | | | Shanxian | 243,854 | 3.621 | 0.905 | 2.556 | 4.218 | 14.922 | 3.391 |
| 0.79 | 379,140 | 10.819 | Linyi | 158,341 | 3.459 | 0.864 | 0.765 | 5.790 | 17.723 | 0.000 |
| | | | Shiliquan | 76,713 | 1.576 | 0.394 | 1.111 | 2.331 | 7.178 | 1.248 |
| | | | Shanxian | 243,854 | 3.621 | 0.905 | 2.556 | 4.218 | 14.922 | 3.391 |
| 0.78 | 379,135 | 10.819 | Linyi | 155,183 | 3.421 | 0.855 | 0.765 | 5.793 | 15.150 | 2.581 |
| | | | Shiliquan | 76,713 | 1.576 | 0.394 | 1.111 | 2.331 | 7.178 | 1.248 |
| | | | Shanxian | 247,699 | 3.659 | 0.915 | 2.582 | 4.261 | 15.075 | 3.426 |
| 0.77 | 377,698 | 10.819 | Linyi | 142,751 | 3.264 | 0.816 | 0.782 | 5.922 | 0.000 | 18.125 |
| | | | Shiliquan | 58,945 | 1.576 | 0.394 | 3.442 | 0.000 | 7.178 | 1.248 |
| | | | Shanxian | 263,709 | 3.815 | 0.954 | 2.692 | 4.444 | 15.721 | 3.573 |

government tax revenue increases from 372,028 $\times 10^3$ CNY to 372,878 $\times 10^3$ CNY. When the sensitivity parameter increases to a certain extent, the government tax revenue no longer increases. The carbon emission quota allocation for each power plant is presented in Table 11.

Therefore, a conclusion can be obtained: As the global sensitivity parameter $\theta$ increases, the conservatism of the government tax revenue obtained under the bi-level BCC model decreases. This confirms that the global sensitivity parameter controls the distance from the uncertain parameter $C_m$ to the inner uncertain set, which means that the requirement of a completely feasible constraint is reduced and the infeasible requirement is relaxed for the solution obtained by considering the uncertain carbon emission parameters $C_m$. The global sensitivity parameter $\theta$, therefore, controls the degree to which constraint violations are allowed. With the increase in $\theta$, the greater the degree of an allowable constraint violation, the greater the scope of allowable infeasibility, and the lower the conservativeness of the solution. However, when the parameter $\theta$ increases to a certain degree, the solution no longer changes.

From Fig. 9, it can be concluded that with the increase in parameter $\theta$, the profit of the Shiliquan power plant first increased from 104,112 $\times 10^3$ CNY to 172,686 $\times 10^3$ CNY and then decreased to 77,610 $\times 10^3$ CNY. In contrast, the profit of the Shanxian power plant first decreased from 199,616 $\times 10^3$ CNY to 149,182 $\times 10^3$ CNY and then increased to 229,140 $\times 10^3$ CNY. In addition, the profit change of the Linyi power plant is relatively small. The largest change is in the Shiliquan power plant, with the highest profit being 55% higher than the lowest profit. When $\theta$ increases to 10$\mathbb{K}$, the profit of each power plant no longer changes.

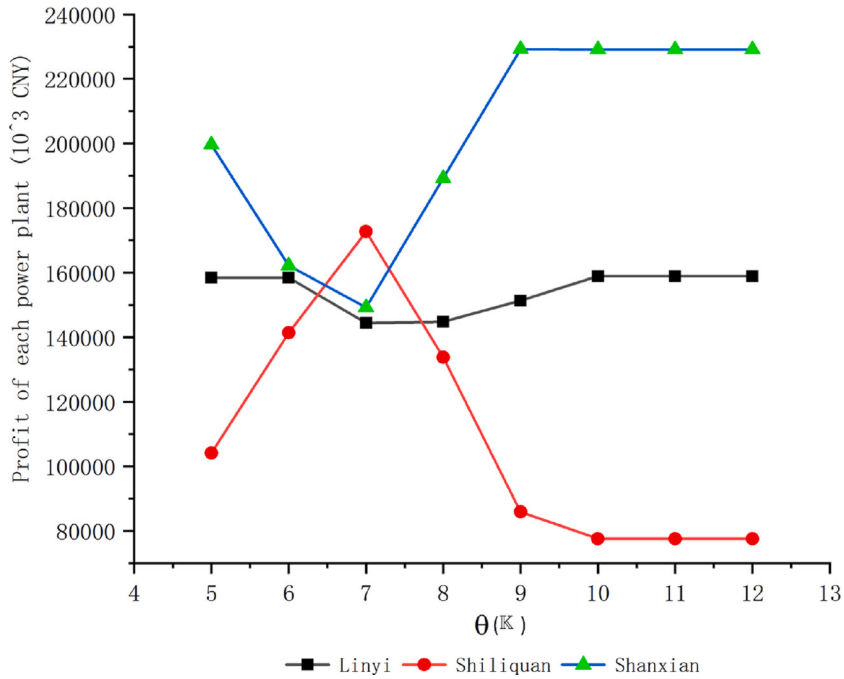


**Fig. 9.** The profit of each power plant under different $\theta$.

**Table 10**
Fuel consumption of each power plant under different models.

| | Power Plant | Fule ($10^5$ tonnes) Straw | Wood | Coal 1 | Coal 2 |
|---|---|---|---|---|---|
| GRC | Linyi | 0.765 | 5.793 | 17.723 | 0.000 |
| | Shiliquan | 1.117 | 2.344 | 7.216 | 1.255 |
| | Shanxian | 2.454 | 4.051 | 14.331 | 3.257 |
| NO | Linyi | 0.765 | 5.793 | 17.723 | 0.000 |
| | Shiliquan | 1.125 | 2.361 | 7.271 | 1.264 |
| | Shanxian | 2.491 | 4.112 | 14.546 | 3.306 |
| RC | Linyi | 0.765 | 5.793 | 14.767 | 2.966 |
| | Shiliquan | 1.108 | 2.326 | 7.163 | 1.246 |
| | Shanxian | 2.448 | 4.041 | 14.296 | 3.249 |

### 5.4.2. The effects of parameter $\tau$

As shown in Fig. 10, as $\tau$ increases from 1.5 to 2.2, the government tax revenue decreases from 372,303 $\times 10^3$ CNY to 371,402 $\times 10^3$ CNY. The carbon emission quota allocation for each power plant is presented in Table 12. The carbon emission quota allocation of each power plant is presented in Table 12.

Therefore, a conclusion can be obtained: As the parameter $\tau$ increases, the conservatism of the decision government tax revenue obtained under the bi-level BCC model increases. The reduction in government tax revenue is reasonable. Parameter $\tau$ controls the size of the inner uncertainty set. With the increase in parameter $\tau$, the perturbation range of carbon emission parameters is larger and the feasible region is smaller, so the decision is more conservative. Therefore, the government tax revenue has decreased.

The profits for each power plant as the parameter $\tau$ varies are given in Fig. 11. As $\tau$ increases, the profits for each power plant decrease. For example, if $\tau$ changes from 1.5 to 2.2, the profit for the Linyi power plant decreases from 158,416 $\times 10^3$ CNY to 158,372 $\times 10^3$ CNY, a reduction of 0.2%. The largest change is for the Shanxian power plant, where the minimum return is reduced by 2417 $\times 10^3$ CNY compared to the maximum return, a 1.5% reduction.

In conclusion, the sensitivity analysis shows that the global sensitivity parameter $\theta$ not only has a significant impact on the government tax revenue compared to parameter $\tau$, but also has a greater impact on the power plant profits. There is a 55% difference between the highest and lowest profits for the Shiliquan power plant under different value of global sensitivity parameters. The difference between the highest and lowest returns for power plants under different values of $\tau$ is not as large. Different parameter settings result in different government tax revenues and different profits for the power plant, and decision-makers can choose the parameters that suit their situation to make their decisions.

## 5.5. Management insights

This case study indicates that our GRC bi-level BCC model has practical guiding significance for the government decision-making and the power plant production planning. Based on the analysis of computational results and sensitivity parameters, several management insights are obtained as follows:

- When decision-makers want to address both the economic objectives of the tax and the impact of environmental damage, the GRC bi-level BCC model can provide some useful instructions. The computational results show that the larger the carbon emission control parameter is, the higher the carbon emissions and the higher the government tax revenue. Therefore, faced with two conflicting objectives, the government policy-makers can choose the appropriate carbon emission control parameters and different value of the carbon intensity control parameters according to different socioeconomic situations.
- Different value of the carbon emission control parameters and the carbon emission intensity parameters have an impact on the decision-making of each power plant. With the reduction of the carbon emission control parameter, the Shanxian power plant is most affected, and its profit decreases the most. Therefore, depending on the government's carbon emission control, power plants are required to change their production plan at any time.
- Compared with the NO model, our GRC bi-level BCC model can effectively resist the influence of uncertain parameters. Even if the determined carbon emission parameters cannot be obtained in the actual production of the power plants, the GRC model can still obtain the optimal solution, and then provide some suggestions for

**Table 11**
Computational results under different value of $\theta$.

| $\theta$ | Government tax revenue ($10^3$ CNY) | Power plant | Profit ($10^3$ CNY) | Free CEQA ($10^6$ tonnes) | Taxable CEQA ($10^6$ tonnes) | Fules | | | |
|---|---|---|---|---|---|---|---|---|---|
| | | | | | | Straw ($10^5$ tonnes) | Wood ($10^5$ tonnes) | Coal 1 ($10^5$ tonnes) | Coal 2 ($10^5$ tonnes) |
| 5 | 372,028 | Linyi | 158,401 | 3.447 | 0.862 | 0.764 | 5.790 | 17.723 | 0.000 |
| | | Shiliquan | 104,112 | 1.838 | 0.459 | 1.302 | 2.732 | 8.415 | 1.463 |
| | | Shanxian | 199,616 | 3.182 | 0.795 | 2.253 | 3.719 | 13.159 | 2.990 |
| 6 | 372,304 | Linyi | 158,416 | 3.444 | 0.861 | 0.764 | 5.790 | 17.723 | 0.000 |
| | | Shiliquan | 141,334 | 2.205 | 0.551 | 1.562 | 3.279 | 10.098 | 1.756 |
| | | Shanxian | 162,210 | 2.817 | 0.704 | 1.998 | 3.298 | 11.669 | 0.265 |
| 7 | 372,465 | Linyi | 144,440 | 3.264 | 0.816 | 0.785 | 5.950 | 0.000 | 18.215 |
| | | Shiliquan | 172,686 | 2.514 | 0.628 | 1.782 | 3.739 | 11.515 | 2.003 |
| | | Shanxian | 189,208 | 3.072 | 0.768 | 2.182 | 3.601 | 12.742 | 2.896 |
| 8 | 372,617 | Linyi | 144,732 | 3.264 | 0.8167 | 0.786 | 5.965 | 0.000 | 18.230 |
| | | Shiliquan | 133,790 | 2.131 | 0.532 | 1.509 | 3.168 | 9.756 | 1.696 |
| | | Shanxian | 189,208 | 3.072 | 0.768 | 2.182 | 3.601 | 12.742 | 2.896 |
| 9 | 372,856 | Linyi | 151,368 | 0.838 | 0.838 | 0.766 | 5.796 | 11.941 | 5.800 |
| | | Shiliquan | 76,713 | 1.576 | 0.394 | 1.111 | 2.331 | 7.178 | 1.248 |
| | | Shanxian | 229,234 | 3.457 | 0.864 | 2.454 | 4.052 | 14.335 | 3.258 |
| 10 | 372,878 | Linyi | 158,467 | 3.435 | 0.858 | 0.764 | 5.790 | 17.723 | 0.000 |
| | | Shiliquan | 77,610 | 1.576 | 0.394 | 1.116 | 2.343 | 7.216 | 1.255 |
| | | Shanxian | 229,140 | 3.455 | 0.863 | 2.454 | 4.051 | 14.331 | 3.257 |
| 11 | 372,878 | Linyi | 158,467 | 3.435 | 0.858 | 0.764 | 5.790 | 17.723 | 0.000 |
| | | Shiliquan | 77,610 | 1.576 | 0.394 | 1.116 | 2.343 | 7.216 | 1.255 |
| | | Shanxian | 229,140 | 3.455 | 0.863 | 2.454 | 4.051 | 14.331 | 3.257 |
| 12 | 372,878 | Linyi | 158,467 | 3.435 | 0.858 | 0.764 | 5.790 | 17.723 | 0.000 |
| | | Shiliquan | 77,610 | 1.576 | 0.394 | 1.116 | 2.343 | 7.216 | 1.255 |
| | | Shanxian | 229,140 | 3.455 | 0.863 | 2.454 | 4.051 | 14.331 | 3.257 |

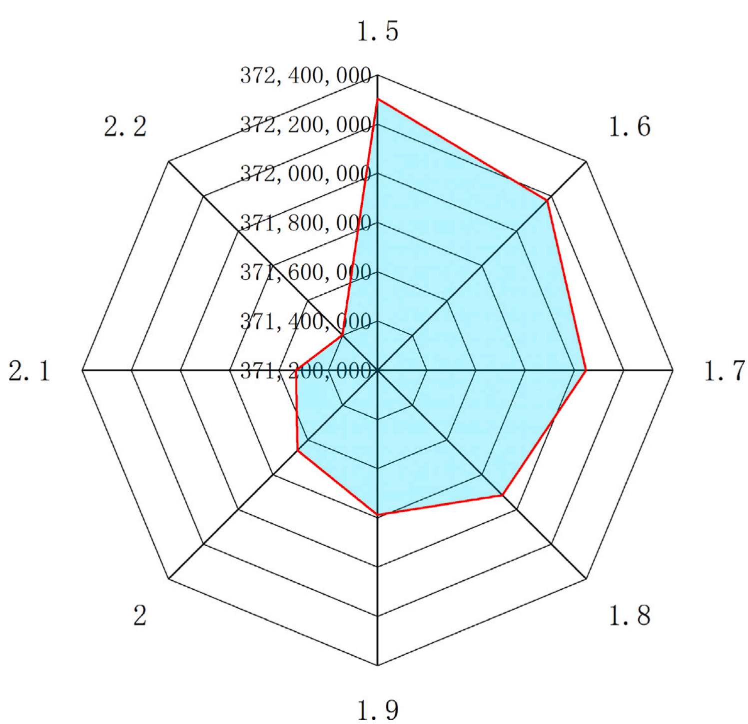


**Fig. 10.** The government tax revenue under different $\tau$.

decision-makers. Compared with the RC model, the GRC bi-level BCC model pays a lower robustness price and is less conservative. Therefore, the GRC model can provide relatively less conservative advice to decision-makers when the determined carbon emission parameters cannot be obtained.

- Sensitivity analysis illustrated that the larger value of the global sensitivity parameter $\theta$, the less conservative the results, i.e., the more the government tax revenue. In addition, the larger the inner uncertainty set parameter $\tau$, the more conservative the results are, i.e., the smaller the government tax revenue. In practice, both

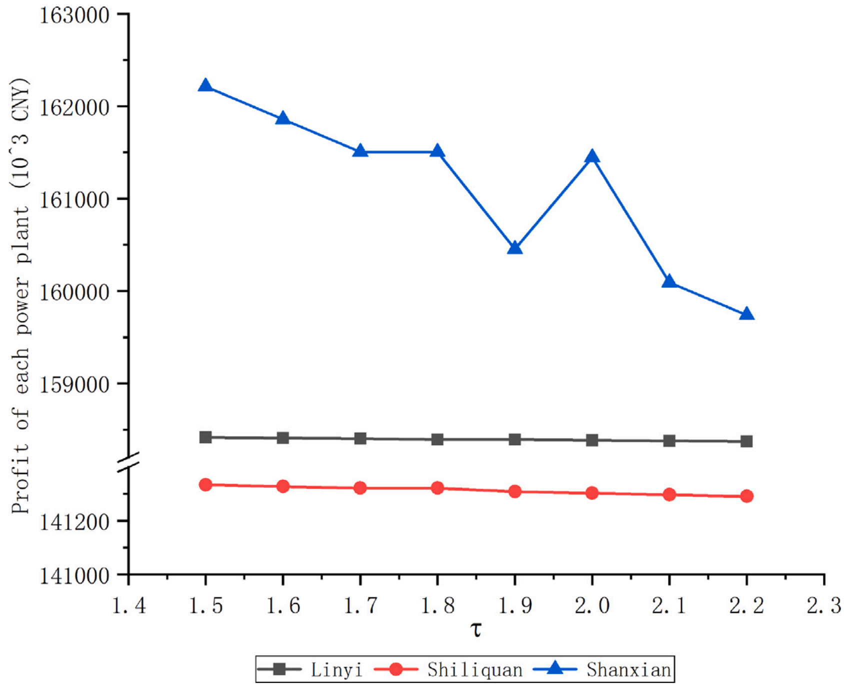


**Fig. 11.** The profit of each power plant under different $\tau$.

**Table 12**
Computational results under different value of $\tau$.

| $\tau$ | Government tax revenue ($10^3$ CNY) | Power plant | Profit ($10^3$ CNY) | Free CEQA ($10^6$ tonnes) | Taxable CEQA ($10^6$ tonnes) | Fules: Straw ($10^5$ tonnes) | Wood ($10^5$ tonnes) | Coal 1 ($10^5$ tonnes) | Coal 2 ($10^5$ tonnes) |
|---|---|---|---|---|---|---|---|---|---|
| 1.5 | 372,303 | Linyi | 158,416 | 3.444 | 0.861 | 0.764 | 5.790 | 17.723 | 0.000 |
| | | Shiliquan | 141,334 | 2.205 | 0.551 | 1.562 | 3.279 | 10.098 | 1.756 |
| | | Shanxian | 162,210 | 2.817 | 0.704 | 1.998 | 3.298 | 11.669 | 2.652 |
| 1.6 | 372,174 | Linyi | 158,410 | 3.446 | 0.861 | 0.764 | 5.790 | 17.723 | 0.000 |
| | | Shiliquan | 141,328 | 2.206 | 0.551 | 1.562 | 3.279 | 10.098 | 1.756 |
| | | Shanxian | 161,857 | 2.815 | 0.703 | 1,996 | 3.284 | 11 655 | 2.648 |
| 1.7 | 372,046 | Linyi | 158,404 | 3.447 | 0.861 | 0.764 | 5.790 | 17.723 | 0.000 |
| | | Shiliquan | 141,322 | 2.207 | 0.551 | 1.562 | 3.279 | 10.098 | 1.756 |
| | | Shanxian | 161,504 | 2.813 | 0.703 | 1.993 | 3.286 | 11.627 | 2.642 |
| 1.8 | 371,917 | Linyi | 158,391 | 3.447 | 0.861 | 0.764 | 5.790 | 17.723 | 0.000 |
| | | Shiliquan | 141,322 | 2.207 | 0.551 | 1.562 | 3.279 | 10.098 | 1.756 |
| | | Shanxian | 161,504 | 2.810 | 0.702 | 1.991 | 3.286 | 11.627 | 2.642 |
| 1.9 | 371,788 | Linyi | 158,391 | 3.447 | 0.861 | 0.764 | 5.790 | 17.723 | 0.000 |
| | | Shiliquan | 141,309 | 2.209 | 0.552 | 1.562 | 3.279 | 10.098 | 1.756 |
| | | Shanxian | 160,445 | 2.808 | 0.702 | 1.988 | 3.282 | 11.614 | 2.639 |
| 2.0 | 371,659 | Linyi | 158,385 | 3.450 | 0.862 | 0.764 | 5.790 | 17.723 | 0.000 |
| | | Shiliquan | 141.303 | 2.210 | 0.552 | 1.562 | 3.279 | 10.098 | 1.756 |
| | | Shanxian | 160.445 | 2.808 | 0.701 | 1.986 | 3.278 | 11.600 | 2.636 |
| 2.1 | 371,530 | Linyi | 158,379 | 3.451 | 0.862 | 0.764 | 5.790 | 17.723 | 0.000 |
| | | Shiliquan | 141,297 | 2.211 | 0.552 | 1.562 | 3.279 | 10.098 | 1.756 |
| | | Shanxian | 160.092 | 2.804 | 0.701 | 1.984 | 3.275 | 11,586 | 2.633 |
| 2.2 | 371,401 | Linyi | 158,372 | 3.452 | 0.863 | 0.764 | 5.790 | 17.723 | 0.000 |
| | | Shiliquan | 141,291 | 2.212 | 0.553 | 1.562 | 3.279 | 10.098 | 1.756 |
| | | Shanxian | 159,739 | 2.802 | 0.700 | 1.981 | 3.271 | 11.572 | 2.630 |

of the parameters can be chosen and adjusted by decision-makers based on their conservatism attitudes, robustness requirements for solutions, and some other presumable information about uncertain parameters.

## 6. Conclusions

This paper investigated the problem of BCC production planning for power plants based on robust carbon emission mechanism. In our problem, the objectives of the government and the power plant are conflicting. The government sought to maximize tax revenue within the limits of the carbon emission control, while the power plant maximized its profit. In addition, during the production process, the power plants were faced with uncertainties, which prompts managers to address new method to deal with these uncertainties.

Based on the questions raised, this paper proposed a GRC bi-level BCC method under robust carbon emission mechanism, where uncertain carbon emission parameters are at the lower level. In our GRC bi-level BCC model, there are two conflicting objectives, this paper adopted a bi-level optimization method to address the hierarchical relationship between the government and the power plant. In the face of uncertainty, this paper employed the budget and box uncertainty sets as inner–outer uncertainty sets to characterize robust carbon emission parameters. Then, using the Lagrangian duality theory, the semi-infinite constraint was transformed into a finite convex constraint system. Finally, the lower-level model was replaced with its equivalent KKT conditions to obtain the single-level biomass–coal co-firing model, which can be solved by convenient solvers like CPLEX.

To demonstrate the effectiveness of the GRC method, the GRC bi-level BCC model was applied to a practical case in Shandong Province China. The computational results demonstrated the credibility of the proposed method in the following aspects:

- The results showed that the increase in carbon emission control parameter $\beta$ leads to an increase in both the government tax revenue and the total carbon emission quota allocation.
- The GRC bi-level BCC model proposed in this paper can effectively resist the influence of uncertain parameters.
- The proposed GRC model is less conservative. The government tax revenue obtained from the GRC model is 2,431,402 CNY higher than that under the RC model.
- With the increase in the global sensitivity parameter $\theta$, the government tax revenue increases.
- As the inner uncertainty set parameter $\tau$ increases, the government tax revenue decreases.

The following aspect can be considered in future research. If the probability distribution information of uncertain parameters is partially known, the distributionally robust optimization method can be used to model our BCC problem, and then decide the CEQA mechanism and the production plan of the power plant.

## CRediT authorship contribution statement

**Jia Zhao:** Conceptualization, Methodology, Writing – original draft, Software, Data curation, Validation. **Yankui Liu:** Supervision, Writing – review & editing, Funding acquisition. **Aixia Chen:** Project administration, Writing – review & editing, Visualization.

## Declaration of competing interest

The authors declare that they have no known competing financial interests or personal relationships that could have appeared to influence the work reported in this paper.

## Data availability

Data will be made available on request.

## Acknowledgments

The authors are grateful to the Editor-in-Chief and anonymous reviewers for their insightful suggestions, which helped us to improve the manuscript significantly. This work is supported by the Natural Science Foundation of Hebei Province, China (No. A2023201020), the Operations Research and Management Innovation Team of Hebei University, China (No. IT2023C02), the National Natural Science Foundation of China (No. 61773150), the Social Science Foundation of Hebei Province, China (No. HB23GL019), and the Post-graduates Innovation Fund Project of Hebei University, China (No. HBU2023SS008).

## Appendix A. Notation and definition of the model.

Notation and definition of the model are shown in this section.

## Appendix B. Proof of Theorem 1

**Proof.** Semi-infinite constraint (5) is equivalently converted to $F(\boldsymbol{z}_m) \leqslant x_m + y_m, \forall m \in \mathcal{M}$ with

$$F(\boldsymbol{z}_m) \equiv \sup_{\boldsymbol{C}_m \in U_2} \{\boldsymbol{C}_m^T \boldsymbol{z}_m - \min_{\boldsymbol{C}'_m \in U_1} \phi(\boldsymbol{C}_m, \boldsymbol{C}'_m)\}, \forall m \in \mathcal{M}.$$

Since the proof is consistent for any $m \in \mathcal{M}$, the following proof will omit $m$ in order to facilitate the representation,

$$\begin{aligned} F(\boldsymbol{z}) &\equiv \sup_{\boldsymbol{C} \in U_2} \{\boldsymbol{C}^T \boldsymbol{z} - \min_{\boldsymbol{C}' \in U_1} \phi(\boldsymbol{C}, \boldsymbol{C}')\} \\ &= \sup_{\boldsymbol{C}' \in U_1, \boldsymbol{C} \in U_2, \boldsymbol{a}, \boldsymbol{b}} \{\boldsymbol{C}^T \boldsymbol{z} - \phi(\boldsymbol{a}, \boldsymbol{b}) | \boldsymbol{a} = \boldsymbol{C}, \boldsymbol{b} = \boldsymbol{C}'\}. \end{aligned}$$

Based on Lagrange duality, we have

$$\begin{aligned} F(\boldsymbol{z}) &= \min_{\boldsymbol{v}, \boldsymbol{d}} \sup_{\boldsymbol{C}' \in U_1, \boldsymbol{C} \in U_2, \boldsymbol{a}, \boldsymbol{b}} \{\boldsymbol{C}^T \boldsymbol{z} - \phi(\boldsymbol{a}, \boldsymbol{b}) - \boldsymbol{v}^T (\boldsymbol{b} - \boldsymbol{C}') - \boldsymbol{d}^T (\boldsymbol{a} - \boldsymbol{C})\} \\ &= \min_{\boldsymbol{v}, \boldsymbol{d}} \{ \sup_{\boldsymbol{C} \in U_2} \{\boldsymbol{C}^T \boldsymbol{z} + \boldsymbol{d}^T \boldsymbol{C}\} + \sup_{\boldsymbol{a}, \boldsymbol{b}} \{-\phi(\boldsymbol{a}, \boldsymbol{b}) - \boldsymbol{v}^T \boldsymbol{b} - \boldsymbol{d}^T \boldsymbol{a}\} \\ &\quad + \sup_{\boldsymbol{C}' \in U_1} \{\boldsymbol{v}^T \boldsymbol{C}'\}\}. \end{aligned}$$

Dividing $F(\boldsymbol{z})$ into three parts, we have $F(\boldsymbol{z}) = \min_{\boldsymbol{v}, \boldsymbol{d}} \{h_1(\boldsymbol{d}, \boldsymbol{z}) + h_2(\boldsymbol{v}, \boldsymbol{d}) + h_3(\boldsymbol{v})\}$ with

$$\begin{aligned} h_1(\boldsymbol{d}, \boldsymbol{z}) &= \sup_{\boldsymbol{C} \in U_2} \{\boldsymbol{C}^T \boldsymbol{z} + \boldsymbol{d}^T \boldsymbol{C}\}, \\ h_2(\boldsymbol{v}, \boldsymbol{d}) &= \sup_{\boldsymbol{a}, \boldsymbol{b}} \{-\phi(\boldsymbol{a}, \boldsymbol{b}) - \boldsymbol{v}^T \boldsymbol{b} - \boldsymbol{d}^T \boldsymbol{a}\}, \\ h_3(\boldsymbol{v}) &= \sup_{\boldsymbol{C}' \in U_1} \{\boldsymbol{v}^T \boldsymbol{C}'\}. \end{aligned}$$

Rewriting the first part yields

$$\begin{aligned} h_1(\boldsymbol{d}, \boldsymbol{z}) &= \sup_{\boldsymbol{C} \in U_2} \{\boldsymbol{C}^T \boldsymbol{z} + \boldsymbol{d}^T \boldsymbol{C}\} \\ &= \sup_{\boldsymbol{C} \in U_2} \{\boldsymbol{C}^T \boldsymbol{z} + \boldsymbol{d}^T \boldsymbol{C} - \delta(\boldsymbol{C} | U_2)\}, \end{aligned}$$

where $\delta(\boldsymbol{C} | U_2)$ is the indicator function of set $U_2$. Based on Fenchel duality, we have

$$h_1(\boldsymbol{d}, \boldsymbol{z}) = \min_{\boldsymbol{e}} \{\delta^*(\boldsymbol{e} | U_2) - [f(\boldsymbol{e}, \boldsymbol{z}) + \boldsymbol{d}^T \boldsymbol{C}]_*\},$$

where $f(\boldsymbol{C}, \boldsymbol{z}) = \boldsymbol{C}^T \boldsymbol{z}$, $\delta^*(\boldsymbol{e} | U_2) = \sup_{\boldsymbol{C} \in U_2} \boldsymbol{C}^T \boldsymbol{e}$ = is the conjugate function of $\delta(\boldsymbol{C} | U_2)$.

According to the relationship between $U_2$ and $\Psi_2$, we obtain $\delta^*(\boldsymbol{e} | U_2) = (\boldsymbol{C}^0)^T \boldsymbol{e} + \delta^*(\boldsymbol{A}^T \boldsymbol{e} | \Psi_2)$ with $\boldsymbol{A} = [\boldsymbol{C}^1, \boldsymbol{C}^2, \ldots, \boldsymbol{C}^L]$ is obtained. Besides, related to the variable $\boldsymbol{e}$, the concave conjugate of the second term in $h_1$ can be derived as follows,

$$h_1(\boldsymbol{d}, \boldsymbol{z}) = \min_{\boldsymbol{e}} \{(\boldsymbol{C}^0)^T \boldsymbol{e} + \delta^*(\boldsymbol{A}^T \boldsymbol{e} | \Psi_2) - f_*(\boldsymbol{e} - \boldsymbol{d}, \boldsymbol{z})\}.$$

The second term $h_2$ in $F(\boldsymbol{z})$ is simplified

$$\begin{aligned} h_2(\boldsymbol{v}, \boldsymbol{d}) &= \sup_{\boldsymbol{a}, \boldsymbol{b}} \{-\phi(\boldsymbol{a}, \boldsymbol{b}) - \boldsymbol{v}^T \boldsymbol{b} - \boldsymbol{d}^T \boldsymbol{a}\} \\ &= \phi^{**}(-\boldsymbol{d}, -\boldsymbol{v}). \end{aligned}$$

Finally, the third term $h_3$ is rewritten as,

$$h_3(\boldsymbol{v}) = \sup_{\boldsymbol{C}' \in U_1} \{\boldsymbol{v}^T \boldsymbol{C}'\} = \delta^*(\boldsymbol{v} | U_1) = (\boldsymbol{C}^0)^T \boldsymbol{v} + \delta^*(\boldsymbol{A}^T \boldsymbol{v} | \Psi_1).$$

Consequently, by substituting $h_i$ into function $F(\boldsymbol{z})$, inequality $F(\boldsymbol{z}) \leqslant x + y$ is equivalent to

$$\begin{aligned} &\min_{\boldsymbol{v}, \boldsymbol{\sigma}} \{\min_{\boldsymbol{e}} \{(\boldsymbol{C}^0)^T \boldsymbol{e} + \delta^*(\boldsymbol{A}^T \boldsymbol{e} | \Psi_2) - f_*(\boldsymbol{e} - \boldsymbol{d}, \boldsymbol{z})\} + \phi^{**}(-\boldsymbol{d}, -\boldsymbol{v}) + (\boldsymbol{C}^0)^T \boldsymbol{v} \\ &\quad + \delta^*(\boldsymbol{A}^T \boldsymbol{v} | \Psi_1)\} \leqslant x + y. \end{aligned}$$

As a result, $F(\boldsymbol{z}) \leqslant \boldsymbol{x} + \boldsymbol{y}$ if and only if there exist $\boldsymbol{v}$, $\boldsymbol{e}$ and $\boldsymbol{d}$ such that

$$(\boldsymbol{C}^0)^T \boldsymbol{e} + \delta^*(\boldsymbol{A}^T \boldsymbol{e} | \Psi_2) - f_*(\boldsymbol{e} - \boldsymbol{d}, \boldsymbol{z}) + \phi^{**}(-\boldsymbol{d}, -\boldsymbol{v}) + (\boldsymbol{C}^0)^T \boldsymbol{v}$$

**Table A.1**
Notation and definition.

| Notation | Definition |
|---|---|
| **Indices** | |
| $m$ | Power plant index, $m \in \mathcal{M} = \{1, 2, \dots, \text{M}\}$, |
| $n$ | Fuel index, $n \in \mathcal{N} = \{1, 2, \dots, \text{N}\}$, 1-$N_a$ represent biomass fuel, $N_{a+1}$-$N$ represent coal fuel, |
| $q$ | Quality index, $q \in \mathcal{Q} = \{1, 2, \dots, \text{Q}\}$, |
| $k$ | Pollutant index, $k \in \mathcal{K} = \{1, 2, \dots, K\}$. |
| **Decision variables** | |
| **Upper level decision variables** | |
| $x_m$ | Free carbon emissions quota allocation for power plant $m$, |
| $y_m$ | Taxable carbon emissions quota allocation for power plant $m$. |
| **Lower level decision variables** | |
| $z_{mn}$ | Amount of fuel $n$ used by power plant $m$. |
| **Deterministic parameters** | |
| GTR | Max government tax revenue, |
| $\rho$ | Value-added tax rate, |
| $P$ | Unit price of electric power, |
| $PC_{mn}$ | Power conversion parameters of fuel n at power plant $m$, |
| $EC_m$ | Electricity consumption rate at power plant $m$, |
| $u_{mn}$ | Unit price of fuel $n$ for power plant $m$, |
| $w$ | Excess carbon emission tax rate, |
| $E$ | Total carbon emissions, |
| $CI$ | Power plant carbon intensity, |
| $r$ | Maximal carbon intensity degree, |
| $FP_m$ | Free carbon emissions quota level for power plant $m$, |
| $\mu$ | Maximal free carbon emissions quota degree, |
| $TCE$ | The cap of carbon emissions, |
| $\beta$ | The carbon emission control parameter, |
| $AQ_m^{min}$ | Minimum allocation quota for power plant $m$, |
| $AQ_m^{max}$ | Maximum allocation quota for power plant $m$, |
| $D_m$ | Basic power demand for power plant $m$, |
| $FA_{mn}$ | Max obtainable amount of fuel $n$ for power plant $m$, |
| $QB_{mq}^L$ | Lower requirements for biomass fuel quality $q$ at power plant $m$, |
| $QB_{mq}^U$ | Upper requirements for biomass fuel quality $q$ at power plant $m$, |
| $QC_{mq}^U$ | Upper requirements for coal fuel quality at power plant $m$, |
| $QC_{mq}^L$ | Lower requirements for coal fuel quality $q$ at power plant $m$, |
| $F_{nq}$ | Property parameters $q$ of fuel $n$, |
| $B_m$ | The upper biomass blending proportion for power plant $m$, |
| $EP_{nk}$ | Unit emission of pollutant $k$ from fuel $n$, |
| $TP_{mk}$ | Unit treatment cost of pollutant $k$ at power plant $m$, |
| $OC_m$ | Operating cost for power plant $m$. |
| **Uncertain parameters** | |
| $C_{mn}$ | Carbon emissions parameter of fuel $n$ at power plant $m$. |

$+\,\delta^*(\boldsymbol{A}^T\boldsymbol{v}|\Psi_1) \leqslant x + y.$

Noting that

$$\begin{aligned}\phi^{**}(-\boldsymbol{d},-\boldsymbol{v}) &= \max_{\boldsymbol{a},\boldsymbol{b}}\{-\boldsymbol{d}^T\boldsymbol{a} - \boldsymbol{v}_T\boldsymbol{b} - \phi(\boldsymbol{a},\boldsymbol{b})\}\\ &\geqslant \max_{\boldsymbol{a}}\{-(\boldsymbol{d}+\boldsymbol{v})^T\boldsymbol{a} - \phi(\boldsymbol{a},\boldsymbol{a})\}\\ &= \max_{\boldsymbol{a}}\{-(\boldsymbol{d}+\boldsymbol{v})^T\boldsymbol{a}\}\\ &= \begin{cases}0, & if \quad \boldsymbol{d} = -\boldsymbol{v},\\ \infty, & if \quad \boldsymbol{d} \neq -\boldsymbol{v},\end{cases}\end{aligned}$$

then we have $\boldsymbol{d} = -\boldsymbol{v}$. By $\phi(\boldsymbol{C}_m, \boldsymbol{C}_m') = \alpha(\|\boldsymbol{C}_m - \boldsymbol{C}_m'\|), \alpha(t) = \theta t, t \geqslant 0$, we have $\phi^{**}(\boldsymbol{v},-\boldsymbol{v}) = \alpha^*(\|\boldsymbol{v}\|_1^*) = 0$ ($\|\cdot\|^*$ denotes the dual norm of $\|\cdot\|$), when $\|\boldsymbol{v}\|_\infty \leqslant \theta$. Noting that $\boldsymbol{d} = -\boldsymbol{v}$ and $f(z) = \boldsymbol{C}^T\boldsymbol{z}$, then one has

$$\begin{aligned}f_*(\boldsymbol{e}-\boldsymbol{d},\boldsymbol{z}) &= f_*(\boldsymbol{e}+\boldsymbol{v},\boldsymbol{z})\\ &= \min_{\boldsymbol{C}}\{\boldsymbol{C}^T(\boldsymbol{e}+\boldsymbol{v}) - \boldsymbol{C}^T\boldsymbol{z}\}\\ &= \begin{cases}0, & if \quad \boldsymbol{e}+\boldsymbol{v} = \boldsymbol{z},\\ -\infty, & if \quad \boldsymbol{e}+\boldsymbol{v} \neq \boldsymbol{z}.\end{cases}\end{aligned}$$

For any $m \in \mathcal{M}$, combined with $f_*(\boldsymbol{e}-\boldsymbol{d},\boldsymbol{z}) = f_*(\boldsymbol{e}+\boldsymbol{v},\boldsymbol{z})$ with $\boldsymbol{e}+\boldsymbol{v} = \boldsymbol{z}$ and $\phi^{**}(\boldsymbol{v},-\boldsymbol{v}) = 0$ with $\|\boldsymbol{v}\|_\infty \leqslant \theta$, then (1) reduces to

$$\begin{cases}(\boldsymbol{C}_m^0)^T\boldsymbol{z}_m + \delta^*(\boldsymbol{A}_m^T(\boldsymbol{z}_m - \boldsymbol{v}_m)|\Psi_2) + \delta^*(\boldsymbol{A}_m^T\boldsymbol{z}_m|\Psi_1) \leqslant \boldsymbol{x}_m + \boldsymbol{y}_m, \forall m \in \mathcal{M},\\ \|\boldsymbol{v}_m\| \leqslant \theta, \forall m \in \mathcal{M}.\end{cases}$$

By the structures of perturbation sets $(\Psi_1, \Psi_2)$, it follows that

$$\delta^*(\boldsymbol{A}_m^T(\boldsymbol{z}_m - \boldsymbol{v}_m)|\Psi_1) = \max_{\zeta\in\Psi_2}\{\boldsymbol{\zeta}^T\boldsymbol{A}_m^T(\boldsymbol{z}_m - \boldsymbol{v}_m)|,$$

$$\|\boldsymbol{\zeta}\|_\infty \leqslant 1\} = \|\boldsymbol{A}_m^T(\boldsymbol{z}_m - \boldsymbol{v}_m)\|_1,$$

$$\delta^*(\boldsymbol{A}_m^T\boldsymbol{z}_m|\Psi_1) = \max_{\zeta'\in\Psi_1}\{(\boldsymbol{\zeta}')^T\boldsymbol{A}_m^T\boldsymbol{v}_m| \quad \|\boldsymbol{\zeta}'\|_\infty \leqslant 1,$$

$$\|\boldsymbol{\zeta}'\|_1 \leqslant \tau\} = \|\boldsymbol{\eta}_m\|_1 + \tau\|\boldsymbol{\Gamma}_m\|_\infty,$$

where $\boldsymbol{\eta}_m + \boldsymbol{\Gamma}_m = \boldsymbol{A}_m^T\boldsymbol{v}_m$.

As a consequence, substituting these expressions, GRC (5) reduces to the system

$$\begin{cases}(\boldsymbol{C}_m^0)^{\mathrm{T}}z_m + \|(\boldsymbol{A}_m^{\mathrm{T}})(\boldsymbol{z}_m - \boldsymbol{v}_m)\|_1 + \|\boldsymbol{\eta}_m\|_1 + \tau\|\boldsymbol{\Gamma}_m\|_\infty\\ \quad \leqslant x_m + y_m, \forall m \in \mathcal{M},\\ \boldsymbol{\eta}_m + \boldsymbol{\Gamma}_m = \boldsymbol{A}_m^{\mathrm{T}}\boldsymbol{v}_m, \forall m \in \mathcal{M},\\ \|\boldsymbol{v}_m\|_\infty \leqslant \theta, \forall m \in \mathcal{M}.\end{cases}$$

**Table C.1**
Sensitivity analysis of global sensitivity parameter $\theta$ under $\mu = 0.82,\ r = 0.77,\ \beta = 0.92$.

| $\theta$ | GTR | Power plant | Profit | Free CEQA | Taxable CEQA | Fules: Straw | Wood | Coal 1 | Coal 2 |
|---|---|---|---|---|---|---|---|---|---|
| | ($10^3$ CNY) | | ($10^3$ CNY) | ($10^6$ tonnes) | ($10^6$ tonnes) | ($10^5$ tonnes) | ($10^5$ tonnes) | ($10^5$ tonnes) | ($10^5$ tonnes) |
| 5 | 368,424 | Linyi | 156,444 | 3.361 | 0.948 | 0.764 | 5.790 | 17.723 | 0.000 |
| | | Shiliquan | 103,069 | 1.791 | 0.505 | 1.302 | 2.732 | 8.414 | 1.463 |
| | | Shanxian | 178,459 | 2.919 | 0.823 | 2.120 | 3.500 | 12.384 | 2.814 |
| 6 | 368,700 | Linyi | 156,229 | 3.355 | 0.946 | 0.764 | 5.790 | 17.533 | 0.190 |
| | | Shiliquan | 140,082 | 2.150 | 0.606 | 1.562 | 3.279 | 10.098 | 1.756 |
| | | Shanxian | 141,543 | 2.566 | 0.723 | 1.867 | 3.082 | 10.906 | 2.478 |
| 7 | 368,914 | Linyi | 141,479 | 3.182 | 0.897 | 0.766 | 5.803 | 5.419 | 12.343 |
| | | Shiliquan | 152,309 | 2.268 | 0.639 | 1.648 | 3.459 | 10.653 | 1.852 |
| | | Shanxian | 147,656 | 2.621 | 0.739 | 1.909 | 3.151 | 11.150 | 2.534 |
| 8 | 369,070 | Linyi | 141,731 | 3.182 | 0.897 | 0.766 | 5.803 | 5.612 | 12.150 |
| | | Shiliquan | 113,632 | 1.894 | 0.534 | 1.376 | 2.888 | 8.894 | 1.546 |
| | | Shanxian | 187,464 | 2.995 | 0.844 | 2.182 | 3.601 | 12.742 | 2.896 |
| 9 | 369,209 | Linyi | 149,465 | 3.268 | 0.921 | 0.765 | 5.796 | 11.941 | 5.800 |
| | | Shiliquan | 76,715 | 1.536 | 0.433 | 1.116 | 2.343 | 7.216 | 1.255 |
| | | Shanxian | 216,268 | 3.266 | 0.921 | 2.379 | 3.927 | 13.895 | 3.157 |
| 10 | 369,221 | Linyi | 156,517 | 3.349 | 0.944 | 0.764 | 5.790 | 17.723 | 0.000 |
| | | Shiliquan | 76,716 | 1.536 | 0.433 | 1.116 | 2.343 | 7.216 | 1.255 |
| | | Shanxian | 207,675 | 3.185 | 0.898 | 2.320 | 3.830 | 13.551 | 3.079 |
| 11 | 369,221 | Linyi | 156,517 | 3.349 | 0.944 | 0.764 | 5.790 | 17.723 | 0.000 |
| | | Shiliquan | 76,716 | 1.536 | 0.433 | 1.116 | 2.343 | 7.216 | 1.255 |
| | | Shanxian | 207,675 | 3.185 | 0.898 | 2.320 | 3.830 | 13.551 | 3.079 |
| 12 | 369,221 | Linyi | 156,517 | 3.349 | 0.944 | 0.764 | 5.790 | 17.723 | 0.000 |
| | | Shiliquan | 76,716 | 1.536 | 0.433 | 1.116 | 2.343 | 7.216 | 1.255 |
| | | Shanxian | 207,675 | 3.185 | 0.898 | 2.320 | 3.830 | 13.551 | 3.079 |

**Table C.2**
Sensitivity analysis of inner uncertainty set parameter $\tau$ under $\mu = 0.82,\ r = 0.77,\ \beta = 0.92$.

| $\tau$ | GTR | Power plant | Profit | Free CEQA | Taxable CEQA | Fules: Straw | Wood | Coal 1 | Coal 2 |
|---|---|---|---|---|---|---|---|---|---|
| | ($10^3$ CNY) | | ($10^3$ CNY) | ($10^6$ tonnes) | ($10^6$ tonnes) | ($10^5$ tonnes) | ($10^5$ tonnes) | ($10^5$ tonnes) | ($10^5$ tonnes) |
| 1.5 | 368,700 | Linyi | 156,229 | 3.355 | 0.946 | 0.764 | 5.790 | 17.533 | 0.190 |
| | | Shiliquan | 140,082 | 2.150 | 0.606 | 1.562 | 3.279 | 10.098 | 1.756 |
| | | Shanxian | 141,543 | 2.566 | 0.723 | 1.867 | 3.082 | 10.906 | 2.478 |
| 1.6 | 368,571 | Linyi | 156,036 | 3.354 | 0.946 | 0.764 | 5.790 | 17.380 | 0.343 |
| | | Shiliquan | 140,076 | 2.151 | 0.606 | 1.562 | 3.279 | 10.098 | 1.756 |
| | | Shanxian | 141,418 | 2.566 | 0.723 | 1.867 | 3.081 | 10.901 | 2.477 |
| 1.7 | 368,442 | Linyi | 156,447 | 3.360 | 0.947 | 0.764 | 5.790 | 17.723 | 0.000 |
| | | Shiliquan | 139,348 | 2.145 | 0.605 | 1.557 | 3.268 | 10.065 | 1.750 |
| | | Shanxian | 141,293 | 2.566 | 0.723 | 1.866 | 3.080 | 10.896 | 2.476 |
| 1.8 | 368,313 | Linyi | 156,440 | 3.361 | 0.948 | 0.764 | 5.790 | 17.723 | 0.000 |
| | | Shiliquan | 139,120 | 2.144 | 0.604 | 1.555 | 3.265 | 10.055 | 1.748 |
| | | Shanxian | 141,169 | 2.566 | 0.723 | 1.865 | 3.078 | 10.891 | 2.475 |
| 1.9 | 368,184 | Linyi | 156,433 | 3.362 | 0.948 | 0.764 | 5.790 | 17.723 | 0.000 |
| | | Shiliquan | 138,892 | 2.143 | 0.604 | 1.554 | 3.261 | 10.045 | 1.746 |
| | | Shanxian | 141,044 | 2.566 | 0.723 | 1.864 | 3.077 | 10.887 | 2.474 |
| 2.0 | 368,055 | Linyi | 156,427 | 3.363 | 0.948 | 0.764 | 5.790 | 17.723 | 0.000 |
| | | Shiliquan | 138,664 | 2.142 | 0.604 | 1.552 | 3.258 | 10.035 | 1.745 |
| | | Shanxian | 140,919 | 2.566 | 0.723 | 1.863 | 3.076 | 10.887 | 2.473 |
| 2.1 | 367,926 | Linyi | 156,420 | 3.365 | 0.949 | 0.764 | 5.790 | 17.723 | 0.000 |
| | | Shiliquan | 138,436 | 2.140 | 0.603 | 1.551 | 3.255 | 10.025 | 1.743 |
| | | Shanxian | 140,794 | 2.566 | 0.723 | 1.862 | 3.074 | 10.887 | 2.473 |
| 2.2 | 367,798 | Linyi | 156,413 | 3.366 | 0.949 | 0.764 | 5.790 | 17.723 | 0.000 |
| | | Shiliquan | 138,209 | 2.139 | 0.603 | 1.549 | 3.252 | 10.015 | 1.741 |
| | | Shanxian | 140,670 | 2.566 | 0.723 | 1.862 | 3.074 | 10.873 | 2.471 |

## Appendix C. Additional sensitivity analysis

### C.1. Sensitivity analysis under $\mu = 0.82,\ r = 0.77,\ \beta = 0.92$

Tables C.1 and C.2 show the sensitivity analyses about the global sensitivity parameter $\theta$ and the inner uncertainty set parameter $\tau$ under $\mu = 0.82,\ r = 0.77,\ \beta = 0.92$, respectively. From Table C.1, we can find that with the increase of global sensitivity parameter $\theta$, there is a non-decreasing trend in the government tax revenue. From Table C.2, the government tax revenue gradually decreases with the increase of the inner uncertainty set parameter $\tau$.

### C.2. Sensitivity analysis under $\mu = 0.78,\ r = 0.79,\ \beta = 0.88$

Tables C.3 and C.4 display the sensitivity analyses about the global sensitivity parameter $\theta$ and the inner uncertainty set parameter $\tau$ under

**Table C.3**
Sensitivity analysis of global sensitivity parameter $\theta$ under $\mu = 0.78$, $r = 0.79$, $\beta = 0.88$.

| $\theta$ | GTR | Power | Profit | Free | Taxable | Fules | | | |
|---|---|---|---|---|---|---|---|---|---|
| | | plant | | CEQA | CEQA | Straw | Wood | Coal 1 | Coal 2 |
| | ($10^3$ CNY) | | ($10^3$ CNY) | ($10^6$ tonnes) | ($10^6$ tonnes) | ($10^5$ tonnes) | ($10^5$ tonnes) | ($10^5$ tonnes) | ($10^5$ tonnes) |
| 5 | 375,404 | Linyi | 151,755 | 3.430 | 0.753 | 0.765 | 5.797 | 10.761 | 6.984 |
| | | Shiliquan | 105,155 | 1.883 | 0.413 | 1.302 | 2.732 | 8.414 | 1.463 |
| | | Shanxian | 231,447 | 3.557 | 0.780 | 2.457 | 4.055 | 12.347 | 3.260 |
| 6 | 375,684 | Linyi | 154,811 | 3.464 | 0.760 | 0.765 | 5.795 | 13.223 | 4.514 |
| | | Shiliquan | 142,586 | 2.260 | 0.496 | 1.562 | 3.279 | 10.098 | 1.756 |
| | | Shanxian | 190,134 | 3.147 | 0.690 | 2.176 | 3.593 | 12.711 | 2.888 |
| 7 | 375,962 | Linyi | 156,316 | 3.479 | 0.763 | 0.765 | 5.793 | 14.429 | 3.304 |
| | | Shiliquan | 180,017 | 2.637 | 0.578 | 1.822 | 3.825 | 11.780 | 2.048 |
| | | Shanxian | 150,708 | 2.755 | 0.604 | 1.909 | 3.151 | 11.150 | 2.534 |
| 8 | 376,122 | Linyi | 155,437 | 3.345 | 0.733 | 0.766 | 5.803 | 5.612 | 12.150 |
| | | Shiliquan | 154,162 | 2.376 | 0.521 | 1.643 | 3.448 | 10.618 | 1.846 |
| | | Shanxian | 190,952 | 3.149 | 0.691 | 2.182 | 3.601 | 12.742 | 2.896 |
| 9 | 376,275 | Linyi | 153,270 | 3.436 | 0.754 | 0.765 | 5.796 | 11.194 | 3.542 |
| | | Shiliquan | 106,018 | 1.892 | 0.415 | 1.308 | 2.745 | 8.453 | 1.470 |
| | | Shanxian | 231,196 | 3.542 | 0.777 | 2.454 | 4.052 | 14.335 | 3.258 |
| 10 | 376,307 | Linyi | 152,089 | 3.422 | 0.751 | 0.765 | 5.797 | 10.986 | 6.759 |
| | | Shiliquan | 78,504 | 1.615 | 0.354 | 1.116 | 2.343 | 7.216 | 1.255 |
| | | Shanxian | 260,940 | 3.833 | 0.841 | 2.656 | 4.384 | 15.512 | 3.525 |
| 11 | 376,307 | Linyi | 152,089 | 3.422 | 0.751 | 0.765 | 5.797 | 10.986 | 6.759 |
| | | Shiliquan | 78,504 | 1.615 | 0.354 | 1.116 | 2.343 | 7.216 | 1.255 |
| | | Shanxian | 260,940 | 3.833 | 0.841 | 2.656 | 4.384 | 15.512 | 3.525 |
| 12 | 376,307 | Linyi | 152,089 | 3.422 | 0.751 | 0.765 | 5.797 | 10.986 | 6.759 |
| | | Shiliquan | 78,504 | 1.615 | 0.354 | 1.116 | 2.343 | 7.216 | 1.255 |
| | | Shanxian | 260,940 | 3.833 | 0.841 | 2.656 | 4.384 | 15.512 | 3.525 |

**Table C.4**
Sensitivity analysis of inner uncertainty set parameter $\tau$ under $\mu = 0.78$, $r = 0.79$, $\beta = 0.88$.

| $\tau$ | GTR | Power | Profit | Free | Taxable | Fules | | | |
|---|---|---|---|---|---|---|---|---|---|
| | | plant | | CEQA | CEQA | Straw | Wood | Coal 1 | Coal 2 |
| | ($10^3$ CNY) | | ($10^3$ CNY) | ($10^6$ tonnes) | ($10^6$ tonnes) | ($10^5$ tonnes) | ($10^5$ tonnes) | ($10^5$ tonnes) | ($10^5$ tonnes) |
| 1.5 | 375,684 | Linyi | 154,811 | 3.464 | 0.760 | 0.765 | 5.795 | 13.223 | 4.514 |
| | | Shiliquan | 142,586 | 2.260 | 0.496 | 1.562 | 3.279 | 10.098 | 1.756 |
| | | Shanxian | 190,134 | 3.147 | 0.690 | 2.176 | 3.593 | 12.711 | 2.888 |
| 1.6 | 375,555 | Linyi | 154,519 | 3.461 | 0.759 | 0.765 | 5.795 | 12.991 | 4.747 |
| | | Shiliquan | 142,580 | 2.261 | 0.496 | 1.562 | 3.279 | 10.098 | 1.756 |
| | | Shanxian | 190,129 | 3.148 | 0.691 | 2.176 | 3.593 | 12.711 | 2.888 |
| 1.7 | 375,426 | Linyi | 154,227 | 3.459 | 0.759 | 0.765 | 5.795 | 12.759 | 4.980 |
| | | Shiliquan | 142,575 | 2.262 | 0.496 | 1.562 | 3.279 | 10.098 | 1.756 |
| | | Shanxian | 190,123 | 3.149 | 0.691 | 2.176 | 3.593 | 12.711 | 2.888 |
| 1.8 | 375,297 | Linyi | 153,935 | 3.457 | 0.758 | 0.765 | 5.795 | 12.527 | 5.212 |
| | | Shiliquan | 142,569 | 2.263 | 0.496 | 1.562 | 3.279 | 10.098 | 1.756 |
| | | Shanxian | 190,117 | 3.150 | 0.691 | 2.176 | 3.593 | 12.711 | 2.888 |
| 1.9 | 375,167 | Linyi | 153,643 | 3.454 | 0.758 | 0.765 | 5.795 | 12.295 | 5.445 |
| | | Shiliquan | 142,563 | 2.264 | 0.497 | 1.562 | 3.279 | 10.098 | 1.756 |
| | | Shanxian | 190,111 | 3.152 | 0.691 | 2.176 | 3.593 | 12.711 | 2.888 |
| 2.0 | 375,038 | Linyi | 153,350 | 3.452 | 0.757 | 0.765 | 5.795 | 12.063 | 5.677 |
| | | Shiliquan | 142,558 | 2.266 | 0.497 | 1.562 | 3.279 | 10.098 | 1.756 |
| | | Shanxian | 190,105 | 3.153 | 0.692 | 2.176 | 3.593 | 12.711 | 2.888 |
| 2.1 | 374,909 | Linyi | 153,058 | 3.450 | 0.757 | 0.765 | 5.795 | 11.831 | 5.910 |
| | | Shiliquan | 142,552 | 2.267 | 0.496 | 1.562 | 3.279 | 10.098 | 1.756 |
| | | Shanxian | 190,099 | 3.154 | 0.692 | 2.176 | 3.593 | 12.711 | 2.888 |
| 2.2 | 374,780 | Linyi | 152,766 | 3.448 | 0.756 | 0.765 | 5.796 | 11.600 | 6.143 |
| | | Shiliquan | 142,547 | 2.268 | 0.497 | 1.562 | 3.279 | 10.098 | 1.756 |
| | | Shanxian | 190,094 | 3.155 | 0.692 | 2.176 | 3.593 | 12.711 | 2.888 |

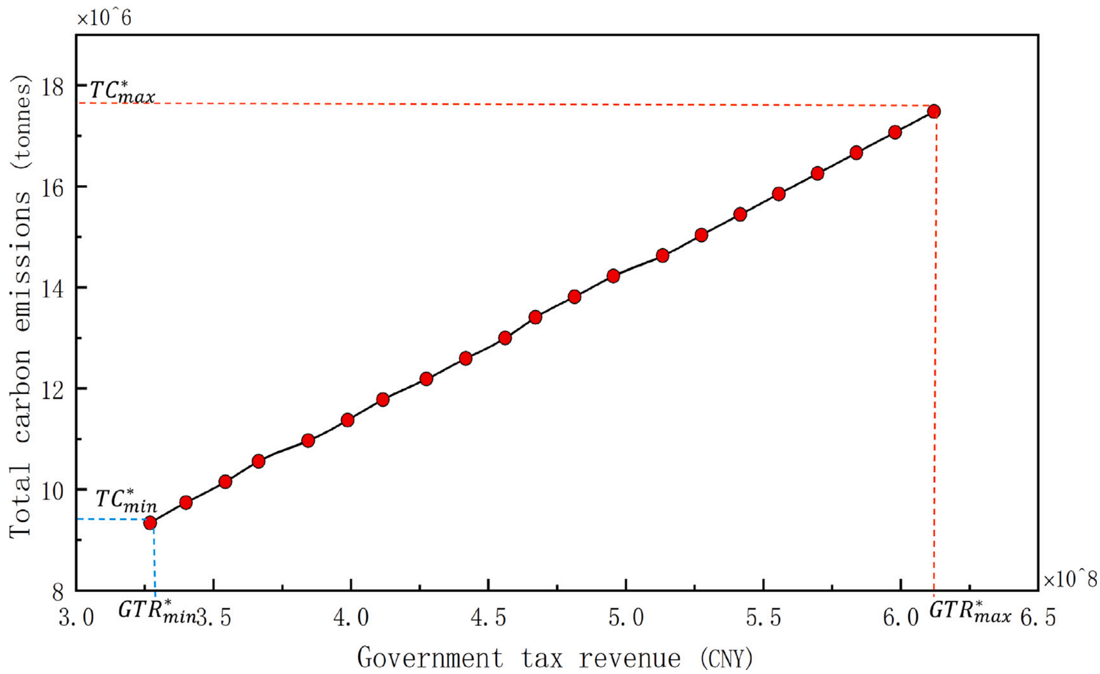


**Fig. D.1.** The Pareto optimal frontier of the bi-objective GRC bi-level BCC model.

**Table D.1**
Payoff table.

| | GTR | TC |
|---|---|---|
| max GTR | $GTR^*_{max}$ | $TC^*_{max}$ |
| min TC | $GTR^*_{min}$ | $TC^*_{min}$ |

**Table D.2**
Payoff table of the bi-objective GRC bi-level BCC model.

| | GTR (CNY) | TC ($10^6$ tonnes) |
|---|---|---|
| max GTR | 611,991,645 | 17.48 |
| min TC | 326,901,964 | 9.34 |

**Table D.3**
Pareto optimal set of the bi-objective GRC bi-level BCC model.

| $i$ | GTR (CNY) | TC ($10^6$ tonnes) | $i$ | GTR (CNY) | TC ($10^6$ tonnes) |
|---|---|---|---|---|---|
| 0 | 326,901,964 | 9.340 | 11 | 481,347,227 | 13.817 |
| 1 | 339,935,594 | 9.747 | 12 | 495,400,783 | 14.224 |
| 2 | 354,301,151 | 10.154 | 13 | 513,369,921 | 14.631 |
| 3 | 366,392,379 | 10.561 | 14 | 527,458,739 | 15.038 |
| 4 | 384,387,862 | 10.968 | 15 | 541,547,557 | 15.445 |
| 5 | 398,753,420 | 11.375 | 16 | 555,636,374 | 15.852 |
| 6 | 411,591,320 | 11.782 | 17 | 569,725,192 | 16.259 |
| 7 | 427,429,541 | 12.189 | 18 | 583,814,010 | 16.666 |
| 8 | 441,759,112 | 12.596 | 19 | 597,902,828 | 17.073 |
| 9 | 456,088,682 | 13.003 | 20 | 611,991,646 | 17.480 |
| 10 | 467,127,132 | 13.410 | | | |

$\mu$ = 0.78, $r$ = 0.79, $\beta$ = 0.88, respectively. As shown in Table C.3, with the increase of global sensitivity parameter $\theta$, the government tax revenue is non-decreasing. From Table C.4, we can find that with the increase of the inner uncertainty set parameter $\tau$, the government tax revenue is gradually decreased.

## Appendix D. Bi-objective GRC bi-level BCC model

On the basis of the maximizing government tax revenue, the second objective of minimizing total carbon emissions (TC) is added in the GRC bi-level BCC model (11) in the main text and the bi-objective GRC bi-level BCC model is constructed, which is as follows:

$$
\begin{aligned}
\max \quad & \mathrm{GTR} = \rho \sum_{m=1}^{M} \sum_{n=1}^{N} [PPC_{mn}(1 - EC_{mn}) - u_{mn} z_{mn}] + w \sum_{m=1}^{M} y_m, \\
\min \quad & \mathrm{TC} = \sum_{m=1}^{M} x_m + y_m, \\
\text{s.t.} \quad & \text{Constraints (1)–(2), (4),} \\
& \max \quad \mathrm{PB}_m = P \sum_{n=1}^{N} PC_{mn}(1 - EC_{mn}) z_{mn} - \sum_{n=1}^{N} u_{mn} z_{mn} \\
& \qquad - \sum_{n=1}^{N} \sum_{k=1}^{K} EP_{nk} TP_{nk} z_{mn} - \\
& \qquad \rho \sum_{m=1}^{M} \sum_{n=1}^{N} [PPC_{mn}(1 - EC_{mn}) - u_{mn}] z_{mn} \\
& \qquad - w \sum_{m=1}^{M} y_m - OC_m, \\
& \text{s.t.} \quad \text{Constraints (5)–(10),}
\end{aligned}
\tag{D.1}
$$

where the constraints in the bi-objective GRC bi-level BCC model are the same as those in the single-objective GRC bi-level BCC model (11) in the main text.

### D.1. Analysis of the bi-objective GRC bi-level BCC model

This section first focuses on transforming model (D.1) into a bi-objective single-level deterministic optimization model, and then applying the augmented $\varepsilon$-constraint method to transform the bi-objective model into a single-objective model.

#### D.1.1. Transforming model (D.1) into a bi-objective single-level deterministic model

The reformation of the semi-infinite constraint in model (D.1) is the same as that in Section 4.1. The transformation of the bi-objective bi-level deterministic optimization model into the bi-objective single-level

**Table D.4**
Computational results of the bi-objective GRC bi-level BCC model in the case of Pareto compromise solution.

| $i$ | GTR | TC | Power plant | Profit | Free CEQA | Taxable CEQA | Fules | | | |
|---|---|---|---|---|---|---|---|---|---|---|
| | | | | | | | Straw | Wood | Coal 1 | Coal 2 |
| | (CNY) | ($10^6$ tonnes) | | ($10^3$ CNY) | ($10^6$ tonnes) | ($10^6$ tonnes) | ($10^5$ tonnes) | ($10^5$ tonnes) | ($10^5$ tonnes) | ($10^5$ tonnes) |
| | | | Linyi | 158,341 | 3.457 | 0.864 | 0.764 | 5.790 | 17.723 | 0.000 |
| 10 | 467,127,132 | 13.410 | Shiliquan | 251,184 | 3.736 | 0.932 | 8.136 | 0.000 | 16.970 | 2.951 |
| | | | Shanxian | 235,409 | 3.539 | 0.884 | 2.497 | 4.123 | 14.486 | 3.315 |

model can refer to Section 4.2. Eventually, the bi-objective single-level BCC deterministic optimization model is obtained as follows:

$$
\begin{aligned}
\max \quad & \mathrm{GTR} = \rho \sum_{m=1}^{M} \sum_{n=1}^{N} [PPC_{mn}(1 - EC_{mn}) - u_{mn} z_{mn}] + w \sum_{m=1}^{M} y_m, \\
\min \quad & \mathrm{TC} = \sum_{m=1}^{M} x_m + y_m \\
\text{s.t.} \quad & \mu_i \in \{0,1\}, \quad i \in \{1,\dots,19\}, \\
& \text{Constraints} \quad (1)\text{–}(2), \quad (4), \quad (6)\text{–}(10), \\
& (14), \quad (16)\text{–}(17), \quad (19).
\end{aligned}
\tag{D.2}
$$

### D.1.2. Transforming model (D.2) into a single objective model

In order to solve model (D.2) effectively, we use the augmented $\varepsilon$-constraint method to transform the bi-objective model into a single objective model in this section. Based on the calculations, a tradeoff between maximizing government tax revenue and minimizing the total carbon emissions is performed. The detailed steps are as follows:

**Step 1:** Choose the government tax revenue (GTR) as the main objective function.

**Step 2:** Obtain the payoff table by solving the single objective optimization problem.

- Taking the first objective GTR without considering the objective of minimizing total carbon emissions, the optimal value $\mathrm{GTR}^*_{max}$ and the optimal solution is obtained. After substituting the optimal solution into the second objective function TC, one gets $\mathrm{TC}^*_{max}$.
- Taking the second objective TC without considering the maximization of the government tax revenue objective, obtain its optimal value $\mathrm{TC}^*_{min}$ and the optimal solution by solving this single objective problem. By substituting the optimal solution, $\mathrm{GTR}^*_{min}$ is obtained.

Therefore, the payoff table is given in Table D.1:

**Step 3:** From Table D.1, we get the range ($\mathrm{TC}^*_{min}$, $\mathrm{TC}^*_{max}$) of the carbon emission objective TC. By dividing the range into $q$ equal intervals, we get $q+1$ demarcation points, from which we get $q+1$ optimization subproblems as follows:

$$
\begin{aligned}
\max_{x,y} \quad & \mathrm{GTR} - \sigma \times \frac{s}{h} \\
\text{s.t.} \quad & \mathrm{TC} - s = \varepsilon_i, \\
& s \in R^+, \\
& \text{Constraints} \quad (1)\text{–}(4), \quad (6)\text{–}(10), \\
& (14), (16)\text{–}(17), (19),
\end{aligned}
\tag{D.3}
$$

where $\sigma \in (10^{-6}, 10^{-3})$ is an adequately small positive number; $s$ is a slack variable; $h = \mathrm{TC}^*_{max} - \mathrm{TC}^*_{min}$ is the range of the second objective TC respectively. In addition, $\varepsilon_i = \mathrm{TC}^*_{max} - \frac{h}{q} \times i \ (i = 0, 1, \dots, q)$ is the $i$th demarcation point of the range ($\mathrm{TC}^*_{min}$, $\mathrm{TC}^*_{max}$) .

**Step 4:** By solving the $q+1$ subproblems in Step 3, we obtain the Pareto optimal solution set.

### D.2. Computational results

Based on the above analysis, we apply the constructed bi-objective GRC bi-level BCC model to the real case about the power plants in Shandong Province in the main text, and get the payoff table, as shown in Table D.2.

In this study, let $q = 20$, and then we get 21 subproblems. By solving these 21 subproblems, we get the Pareto optimal solutions of the bi-objective GRC bi-level BCC model as shown in Table D.3. Visualizing the obtained Pareto optimal solutions, Fig. D.1 displays the Pareto optimal frontier of the developed bi-objective model. From the results plotted in Fig. D.1, we can find that with the increase of government tax revenue, the total carbon emissions also increase, which indicates that the objectives of maximizing government tax revenue and minimizing carbon emissions are in conflict with each other.

Furthermore, we choose the compromise solution from all the Pareto optimal solutions in accordance with the principle of equal importance of the two conflicting objectives, which is Pareto point $i = 10$. Table D.4 shows in the case of the Pareto compromise solution, the free CEQA and taxable CEQA allocated by the government to every power plant, as well as the production planning decisions of each power plant.

## References


Allman, A., Lee, C., Martn, M., Zhang, Q., 2021. Biomass waste-to-energy supply chain optimization with mobile production modules. Comput. Chem. Eng. 150, 107326. http://dx.doi.org/10.1016/j.compchemeng.2021.107326.

Aranguren, M.F., Castillo-Villar, K.K., 2022. Bi-objective stochastic model for the design of large-scale carbon footprint conscious co-firing biomass supply chains. Comput. Ind. Eng. 171, 108352. http://dx.doi.org/10.1016/j.cie.2022.108352.

Aviso, K.B., Sy, C.L., Tan, R.R., Ubando, A.T., 2020. Fuzzy optimization of carbon management networks based on direct and indirect biomass co-firing. Renew. Sustain. Energy Rev. 132, 110035. http://dx.doi.org/10.1016/j.rser.2020.110035.

Awudu, I., Zhang, J., 2012. Uncertainties and sustainability concepts in biofuel supply chain management: A review. Renew. Sustain. Energy Rev. 16, 1359–1368. http://dx.doi.org/10.1016/j.rser.2011.10.016.

Ben-Tal, A., El Ghaoui, L., Nemirovski, A., 2009. Robust Optimization. Princeton University Press, http://dx.doi.org/10.1515/9781400831050.

Bertsimas, D., Sim, M., 2004. The price of robustness. Oper. Res. 52, 35–53. http://dx.doi.org/10.1287/opre.1030.0065.

Chen, A., Liu, Y., 2023a. Designing globalized robust supply chain network for sustainable biomass-based power generation problem. J. Clean. Prod. 413, 137403. http://dx.doi.org/10.1016/j.jclepro.2023.137403.

Chen, A., Liu, Y., 2023b. Optimizing sustainable biomass-coal co-firing power plant location problem under ambiguous supply. Comput. Ind. Eng. 182, 109401. http://dx.doi.org/10.1016/j.cie.2023.109401.

Cutz, L., Berndes, G., Johnsson, F., 2019. A techno-economic assessment of biomass co-firing in czech Republic, France, Germany and Poland. Biofuels, Bioprod. Biorefin. 13, 1289–1305. http://dx.doi.org/10.1002/bbb.2034.

Ekşioğlu, S.D., Karimi, H., Ekşioğlu, B., 2016. Optimization models to integrate production and transportation planning for biomass co-firing in coal-fired power plants. Iie Trans. 48, 901–920. http://dx.doi.org/10.1080/0740817X.2015.1126004.

Feng, Z., Tang, W., Niu, Z., Wu, Q., 2018. Bi-level allocation of carbon emission permits based on clustering analysis and weighted voting: a case study in China. Appl. Energy 228, 1122–1135. http://dx.doi.org/10.1109/TPWRS.2009.2030377.

Fujishima, H., Yoshioka, Y., Kuroki, T., Tanaka, A., Otsuka, K., Okubo, M., 2011. Development of low-emission bio-fuel boiler system with plasma-chemical hybrid $NO_x$ reduction. IEEE Trans. Ind. Appl. 47, 2210–2217. http://dx.doi.org/10.1109/TIA.2011.2161852.

Gebreslassie, B.H., Yao, Y., You, F., 2012. Multiobjective optimization of hydrocarbon biorefinery supply chain designs under uncertainty. In: 2012 IEEE 51st IEEE Conference on Decision and Control (CDC). IEEE, pp. 5560–5565. http://dx.doi.org/10.1109/CDC.2012.6426661.

Global, Bp., 2021. Bp statistical review of world energy. 2022. https://www.bp.com/content/dam/bp/business-sites/en/global/corporate/pdfs/energy-economics/statistical-review/bp-stats-review-2022-full-report.pdf (accessed 20 2022).

Global Energy Review, 2021. Global energy review: $CO_2$ emissions in 2021. https://www.iea.org/reports/global-energy-review-co2-emissions-in-2021-2 (accessed 21 2022).

Huang, Q., Xu, J., 2020. Bi-level multi-objective programming approach for carbon emission quota allocation towards co-combustion of coal and sewage sludge. Energy 211, 118729. http://dx.doi.org/10.1016/j.energy.2020.118729.

Jones, B., Keen, M., Strand, J., 2013. Fiscal implications of climate change. Int. Tax Public Finance 20, 29–70. http://dx.doi.org/10.1007/s10797-012-9214-3.

Karimi, H., Ekşioğlu, S.D., Carbajales-Dale, M., 2021. A biobjective chance constrained optimization model to evaluate the economic and environmental impacts of biopower supply chains. Ann. Oper. Res. 296, 95–130. http://dx.doi.org/10.1007/s10479-019-03331-x.

Khademi, A., Ekşioğlu, S., 2021. Optimal governmental incentives for biomass cofiring to reduce emissions in the short-term. IISE Trans. 53, 883–896. http://dx.doi.org/10.1080/24725854.2020.1718247.

Kim, J., Realff, M.J., Lee, J.H., 2011. Optimal design and global sensitivity analysis of biomass supply chain networks for biofuels under uncertainty. Comput. Chem. Eng. 35, 1738–1751. http://dx.doi.org/10.1016/j.compchemeng.2011.02.008.

Li, B., Boyabatlı, O., Avcı, B., 2023. Economic and environmental implications of biomass commercialization in agricultural processing. Manage. Sci. 69, 3561–3577. http://dx.doi.org/10.1287/mnsc.2022.4518.

Lima, C., Relvas, S., Barbosa-Pvoa, A., 2021. Designing and planning the downstream oil supply chain under uncertainty using a fuzzy programming approach. Comput. Chem. Eng. 151, 107373. http://dx.doi.org/10.1016/j.compchemeng.2021.107373.

Nussbaumer, T., 2003. Combustion and co-combustion of biomass: fundamentals, technologies, and primary measures for emission reduction. Energy Fuels 17, 1510–1521. http://dx.doi.org/10.1021/ef030031q.

Oberschelp, C., Pfister, S., Raptis, C.E., Hellweg, S., 2019. Global emission hotspots of coal power generation. Nat. Sustain. 2, 113–121. http://dx.doi.org/10.3929/ethz-b-000324460.

Ooi, W.J., How, B.S., Ng, D.K., Ng, L.Y., Andiappan, V., 2022. Analysing the impact of stakeholder relationships in the optimisation of biomass supply chains. Comput. Chem. Eng. 168, 108035. http://dx.doi.org/10.1016/j.compchemeng.2022.108035.

Samani, M.R.G., Hosseini-Motlagh, S.M., 2021. A mixed uncertainty approach to design a bioenergy network considering sustainability and efficiency measures. Comput. Chem. Eng. 149, 107305. http://dx.doi.org/10.1016/j.compchemeng.2021.107305.

San Juan, J.L.G., Sy, C.L., 2022. Multi-objective robust optimization for the design of biomass co-firing networks. In: Intelligent Engineering and Management for Industry 4.0. pp. 159–168. http://dx.doi.org/10.1007/978-3-030-94683-8_15.

Shabani, N., Sowlati, T., 2016. A hybrid multi-stage stochastic programming-robust optimization model for maximizing the supply chain of a forest-based biomass power plant considering uncertainties. J. Clean. Prod. 112, 3285–3293. http://dx.doi.org/10.1016/j.energy.2014.10.019.

Sinha, A., Malo, P., Deb, K., 2017. A review on bilevel optimization: From classical to evolutionary approaches and applications. IEEE Trans. Evol. Comput. 22, 276–295. http://dx.doi.org/10.1109/TEVC.2017.2712906.

Soren, A., Shastri, Y., 2019. Resilient design of biomass to energy system considering uncertainty in biomass supply. Comput. Chem. Eng. 131, 106593. http://dx.doi.org/10.1016/j.compchemeng.2019.106593.

Sun, R., Liu, T., Chen, X., Yao, L., 2021. A biomass-coal co-firing based bi-level optimal approach for carbon emission reduction in China. J. Clean. Prod. 278, 123318. http://dx.doi.org/10.1016/j.jclepro.2020.123318.

Theozzo, B., dos Santos, M.T., 2023. A robust optimization framework for forest biorefineries design considering uncertainties on biomass growth and product selling prices. Comput. Chem. Eng. 175, 108256. http://dx.doi.org/10.1016/j.compchemeng.2022.107693.

Varshney, D., Mandade, P., Shastri, Y., 2019. Multi-objective optimization of sugarcane bagasse utilization in an Indian sugar mill. Sustain. Prod. Consum. 18, 96–114. http://dx.doi.org/10.1016/j.spc.2018.11.009.

Wang, X., Fan, F., Liu, C., Han, Y., Liu, Q., Wang, A., 2022. Regional differences and driving factors analysis of carbon emissions from power sector in China. Ecol. Indic. 142, 109297. http://dx.doi.org/10.1016/j.ecolind.2022.109297.

Xu, J., Huang, Q., Lv, C., Feng, Q., Wang, F., 2018. Carbon emissions reductions oriented dynamic equilibrium strategy using biomass-coal co-firing. Energy Policy 123, 184–197. http://dx.doi.org/10.1016/j.enpol.2018.08.043.

Yang, F., Lee, H., 2022. An innovative provincial $CO_2$ emission quota allocation scheme for Chinese low-carbon transition. Technol. Forecast. Soc. Change 182, 121823. http://dx.doi.org/10.1016/j.techfore.2022.121823.

Zhang, L., Li, Y., Jia, Z., 2018. Impact of carbon allowance allocation on power industry in Chinas carbon trading market: Computable general equilibrium based analysis. Appl. Energy 229, 814–827. http://dx.doi.org/10.1016/j.apenergy.2018.08.055.

Zhao, S., Shi, Y., Xu, J., 2018. Carbon emissions quota allocation based equilibrium strategy toward carbon reduction and economic benefits in China's building materials industry. J. Clean. Prod. 189, 307–325. http://dx.doi.org/10.1016/j.jclepro.2018.03.073.

Zhou, X., James, G., Liebman, A., Dong, Z.Y., Ziser, C., 2009. Partial carbon permits allocation of potential emission trading scheme in Australian electricity market. IEEE Trans. Power Syst. 25, 543–553. http://dx.doi.org/10.1109/TPWRS.2009.2030377.

Zhou, P., Wang, M., 2016. Carbon dioxide emissions allocation: A review. Ecol. Econom. 125, 47–59. http://dx.doi.org/10.1016/j.ecolecon.2016.03.001.

Zhu, N., Bu, Y., Jin, M., Mbroh, N., 2020. Green financial behavior and green development strategy of Chinese power companies in the context of carbon tax. J. Clean. Prod. 245, 118908. http://dx.doi.org/10.1016/j.jclepro.2019.118908.